NORM FASTENERS
AR-GE MERKEZİ YAYINLARI

R&D CENTER PUBLICATIONS

2017

VOLUME 3

NORM
FASTENERS

NORM FASTENERS
AR-GE MERKEZİ YAYINLARI
R&D CENTER PUBLICATIONS

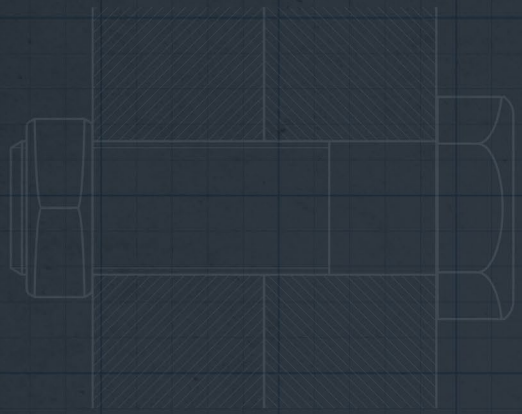

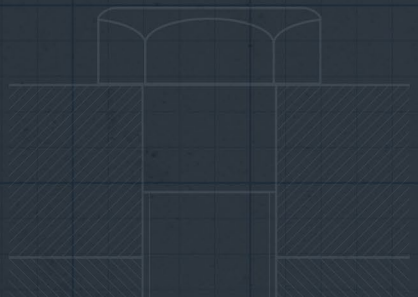

TOOL LIFE ENHACEMENT IN COLD BOLT FORGING PROCESS: EFFECT OF FORGING STAGE DESIGN

CIVATA SOĞUK DÖVME İŞLEMİNDE KALIP ÖMRÜNÜN ARTTIRILMASI: DÖVME KADEME TASARIMININ ETKİSİ

Cenk KILIÇASLAN
Umut İNCE

Sakarya Üniversitesi
Fen Bilimleri Enstitüsü Dergisi

Tool Life Enhacement In Cold Bolt Forging Process: Effect Of Forging Stage Design

Civata Soğuk Dövme İşleminde Kalıp Ömrünün Arttırılması: Dövme Kademe Tasarımının Etki

Cenk Kılıçaslan*[1]
Umut İnce[2]

Norm Cıvata San. ve Tic. A.Ş., Turkey (Norm Fasteners)

*** Sorumlu Yazar / Corresponding Author**

[1] Dr. Cenk Kılıçaslan Norm Cıvata San. ve Tic. A.Ş., 10007 Sok. No:1/1 A.O.S.B. 35620 Çiğli/İzmir
[2] Umut İnce Norm Cıvata San. ve Tic. A.Ş., 10007 Sok. No:1/1 A.O.S.B. 35620 Çiğli/İzmir

ÖZET

Bu çalışmada özel M10x32 dog-point cıvataların soğuk dövme işleminde meydana gelen kalıp hasarı Simufact.forming sonlu elemanlar simülasyon programı kullanılarak incelenmiş ve dövme kademe tasarımlarında değişimler yapılarak kalıplar üzerinde meydana gelen yüksek gerilme değerlerinin azaltılması amaçlanmıştır. Çalışmanın ilk kısmında cıvataya ait beş farklı dövme kademesinde meydana gelen malzeme akışı modellenerek belirlenmiş, kalıp kırılmasının yaşandığı dövme kademesinde oluşan kontak basınçları ile kalıp gerilmeleri tespit edilmiştir. Simülasyonlar cıvata kafa ve flanş kısmının dogpoint'in oluşturulduğu dövme kademesinde aynı anda şekillendirilmesi nedeniyle sabit kalıp üzerinde yüksek çekme gerilmesinin oluştuğunu ve kalıbın bu nedenle hasara uğradığını tespit etmiştir. Bu durumu engellemek amacıyla dog-point kısmı bir sonraki dövme kademesine alınmış ve hazırlık açısı 40°'ye düşürülmüştür. Buna ek olarak tek parça olan dövme kalıbı tasarımı iki parçalı tasarım ile değiştirilmiştir. Bu tasarımlar ile gerçekleştirilen simülasyonlar dövme kalıbındaki gerilmenin yaklaşık %70 oranında azaldığını göstermiştir. Son olarak yenilenen kalıplar ile yapılan üretim denemelerinde kalıp ömrünün 3.8 kat arttığı görülmüştür.

Anahtar Kelimeler: Soğuk dövme, cıvata, simülasyon, kalıp, hasar

ABSTRACT

In this paper, tool failure evolution in cold forging process of special M10x32 dog-point bolts was investigated with Simufact.forming finite element software. In the first part of the study, material flow in the five different forging stages were modeled and contact and tool stresses were determined. Simulations revealed that simultaneous forming of the flange, head and socket of the bolt with dog-point section causes excessive tensile stress evolution on the stationary die which leads to tool fracture. To prevent the failure, forming of dog-point section was shifted to further forging stage and preparation angle for dog-point was decreased to 40°. In addition, monolithic tool design was replacaed with split insert design. Simulations
carried out with these designs showed that tool stress was decreased about 70%. Finally, forging trials were also conducted with the updated tools and tool life was seen to increase about 3.8 times.

Keywords: Cold forging, bolt, simulation, tool, failure

1. INTRODUCTION

Cold forging is a metal forming process which enables high speed mass production with great mechanical properties. Leading automobile companies starts to prefer complex forged parts for their superior mechanical properties over cast and machined parts [1]. This forces forging companies to decrease production costs. Due to increasing geometrical complexity of the parts, forging tools (dies) are exposed to excessive forming loads which negatively affects service life of tools. Strain hardening of workpiece material, extreme friction conditions, high strain rates and poor lubrication are also triggers of tool failure. In cold forging tools, main failure mechanisms can be listed as; i) plastic deformation, ii) wear and iii) fatigue [2, 3]. In cold forging process, dies and punches are subjected to compressive stresses up to 2000 MPa that may lead plastic deformations like chipping and local fractures. In some cases, complete bending of a punch may happen. For these reasons, high compressive strength and hardness are required for tool materials [4]. Wear is the loss of the material from the parts that are in contact due to excessive friction under high normal stress. In metal forming operations, wear has a great influence on tool life, dimensional accuracy and surface quality of products [5]. Dynamic and repeated forging of workpiece material causes cycling loading on forging dies and it may lead crack initiation and early fracture of the die which is classified as fatigue failure [6]. More information about failure of dies and molds can be found in the review paper of Jhavar, Paul and Jain [7]. Tool life has significant impact on forging cost in fastener production. As cold forging tool costs cover 10% for standard and 40% for special bolts of total production cost, it is crucial to improve tool life to increase competitiveness of the company. It is also important to decrease inactive time of the forging press due to replacing of failed dies, labor efforts and energy. At this point, quick application of finite element simulations of metal forging operations becomes very valuable in order to make design modifications to increase the effectiveness of the dies. In metal forming industry, researches were mainly focused on numerical modeling of forming processes. Simulations has been used in German and American forging industry since 1980s [8]. Industrial and scientific applications of metal forming simulations grew with the development of commercial finite element softwares in 1990s. Metal forming simulation softwares like Simufact.forming, SFTC Deform, Forge NxT and Qform are leading examples. By the help of these softwares, stress distribution can be determined on tools and results of critical design modifications can be obtained without conducting any trial-error studies in the production. In the literature, studies are mainly focused on tool life estimation, effects of die surface modifications to improve tool life, failure mechanisms and shrink fitting effects on the tool stresses. Geiger et al. [9] investigated Von-mises tress distribution in extrusion process and they used numerical results to obtain optimum die shoulder geometry. It was concluded that Vonmises stress on the die was reduced to 1050 MPa from 1535 MPa with the usage of optimum radius value in extrusion die. Berns et al. [10] determined the critical stress area on dies in the process of screw forging. Particle distribution in metal matrix of forging die was then optimized by using microscale simulations to get highest cracking resistance. Double dispersed tool material was found to be 30% higher fracture toughness in
contrast to single dispersion material. Vazquez et al. [11] revealed the potential of different methods to improve tool life in cold forging. Usage of tougher insert material, increasing shrink fit ratio and splitting insert from the locations where the maximum principle stress is highest were determined to be very effective on tool life enhancement. Engel and Popp [12] applied excimer laser to surface of cold forging die to form microtextures. It was found that microtextures provide extra space for lubrication in contrast to polished surfaces and the tool life was increased up to 300%. Lee et al. [13] investigated the effect of shrink fitting ratios on the effective stress generated on cold forging dies in the process of hexagonal bolt and gear forming. Optimum shrink fitting ratios were 0.52 and 0.75% for first two bolt forging stages and 0.33% for gear forging. It was also concluded that appropriate shrink fitting ratio should be determined for each operation to get high cycle fatigue tool life. Andreas et al. [4] investigated the effects of surface finishing operation on tribological properties of G55 cemented carbide. After EDM (Electric discharge machining), tool surface was shot peened and polished with diamond grits having 15 µm (D15), 9 µm (D9), 6 µm (D6) and 1 µm (D1). It was determined that polishing up to D6 leads to reduce friction factor to 0.03 while polishing with D1 does not have any influence on friction factor. It is also important to note that decrease in surface roughness may cause to reduce oil retaining ability of the surface which results an increase in friction. Ku and Kang [1] modeled the multi-stage cold forging process of steel outer race of BJ-type CV joint and determined the tool stresses. Experimental application of the process revealed that part was well formed with desired dimensions
without experiencing any tool failure. It was concluded that results of the numerical simulation was very applicable. Ku and Kang [14] used numerical forming simulations to investigate flow of inner race with ball grove parts. Tool failure was detected after forging of 15 parts. Tool stress analysis were carried out with Deform software and tool modification, increasing tool fillet radius from 1 to 100 mm, was seen to decrease tool stress about 70%. Yurtdaş et al. [15] revealed the potential usage of carbon fiber reinforced composite tubes as stress rings in cold forging dies. Study showed that shrink fitting ratio can be increased up to 3.5% with carbon fiber composites while conventional tool steel stress rings allows maximum 0.7% shrink fitting ratios. In this paper, multi-stage cold forging process of special M10x32 dog-point bolts was investigated numerically to reveal the reasons of tool failure occurred in fourth forging stage of the operation. Forging simulations and tool analyses were carried out in Simufact.forming finite element software. Material flow in the five different forging stages, contact and tool stresses were determined. Modifications were made in die geometry and forming simulations were repeated to reduce tool stresses.

2. COLD FORGING PROCESS AND TOOL FAILURE

M10x32 dog-point bolts were forged from annealed DIN 1.5536 steel alloy on a forging press having maximum capacity of 1395 kN (140 tones) in Norm Fasteners Co./Turkey. Forging stages and final bolt geometry before threading process (Stage 5) are shown in Figure 1. The bolt is forged to desired geometry and dimensions through using five forging stages. The process begins with the shearing of the work-piece material from a continuous bar. Work-piece is then transferred to stage 1 by grippers. Top die pushes the work-piece and forces it to flow through stationary die cavity. After finishing the forming stroke, ejector pushes the formed part and throw it through the outside of the die. Grippers again hold the formed part and transfer it to the

next forging stage. As shown in Figure 1, extrusion process is conducted in stage 1. Furthermore, head section of the part is prepared for hexagonal shape in stage 2. The initial hexagonal shape is given to the part in stage 3. In stage 4, socket, flange and dog-point in the shaft is formed. At final stage reduction in the shaft is formed.

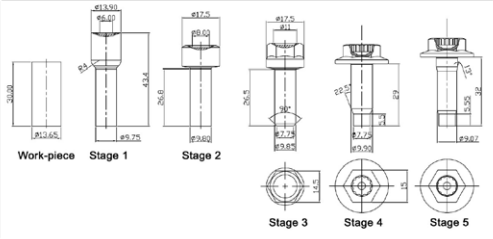

Fig. 1 Forging stages of M10x32 dog-point bolt.

Technical drawing of stage 4 die couple is shown in Figure 2(a). Die system consists of moving and stationary die. Tool failure was seen on the die number 4 which forms dog-point section on the shaft. The picture of the failed tool is shown in Figure 2(b). As depicted in the figure, fracture started from the tool radius and propagated longitudinally though the outer diameter of the WC-Co insert. Surface cracking was also seen inside the tool cavity as depicted with the arrows in Figure 2(b). This type of failure seen on the forging tools is classified as forced ruptures and caused by excessive forging loads [16]. Because of that, forging load and tool stress distribution have to be investigated.

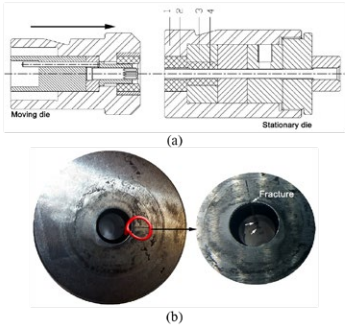

Fig. 2 (a) Die system of stage 4; moving and stationary die, (b) the picture of fractured tool.

3. NUMERICAL MODELS

Numerical models of cold forging operation were prepared in Simufact.forming finite element software. Mechanical models were also coupled with thermal analysis to consider temperature effects on flow stress of the workpiece material. Examples of numerical models are shown in Figure 3. Stage 1 and 2 were simulated with 2D models due to the axisymmetry while 3D models were used for stage 3, 4 and 5. As shown in the figure, numerical models consist of stationary and moving dies and the workpiece. Dies were modeled as rigid. Due to high speed of the forging process, no heat transfer was defined between dies and workpiece. Workpiece material, DIN 1.5536, was modeled as plastic material and true stress- true plastic strain curves between temperatures of 20 an 400°C and strain rates between 1 and 50s^{-1} was defined to the software. In 2D models, 5,000 quad elements were used in the mesh of the workpiece. In 3D models, half of the semi-formed part was modeled and symmetry plane was defined to decrease calculation time. Non-homogenous mesh distribution was used in 3D models. Smaller elements were used on the main deformation areas as depicted in Figure 3(b) and total 28,000 hex elements were used in the finite element mesh. Proper modeling of friction is crucial to get realistic material flow in metal forming simulations. In this study, temperature dependent Coloumb friction coefficient was defined to the software.

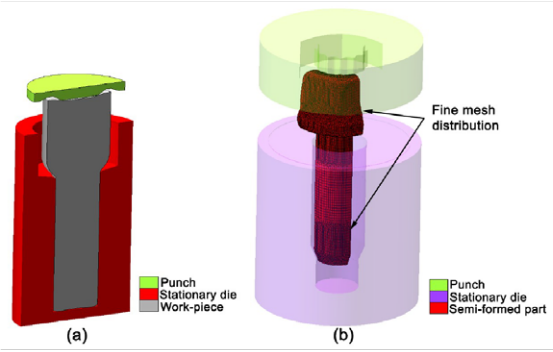

Fig. 3 Examples of numerical models; (a) 2D axisymmetric and (b) 3D models.

After conducting forming simulations, tool stress analysis were carried out for stage 4. Numerical model of stationary die system is shown in Figure 4. Tool numbers in the figure are same with the ones depicted in Figure 2(a). Here, no.1 and no.3 are stress rings made of DIN 1.2344 while no.2 and no.4 are inserts made of WC-27%Co (G55).

In the numerical model, stress rings and insets were assumed to be elastic materials. Elastic modulus and poisson's ratio of DIN 1.2344 and G55 are 215 GPa and 0.3 and 450 GPa and 0.22, respectively. The tensile strength of DIN 1.2344 is about 1380 MPa. Due to fracture evolution on no.4 insert, compressive (3000 MPa) and tensile strength (700 MPa) of G55 material were used failure criteria. Shrink fit was also considered in the tool stress analysis and 0.5% shrink fitting ratio was applied between stress rings and inserts. In the numerical model, dies no.3 and no.4 were fixed from the their lower surfaces in all directions and rotations. The forging force determined from forming simulations was applied to the elastic dies. Tetrahedral elements were used in the finite element meshes of inserts and stress rings. Each insert and stress ring consist of 154,000 and160,000 tetra elements, respectively. Fine mesh distributions were used on the fracture locus.

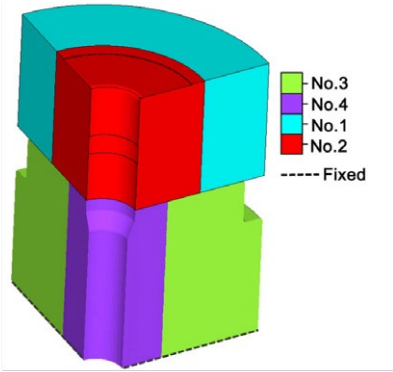

Fig. 4 Numerical model of tool stress analysis in stage 4.

4. RESULTS AND DISCUSSIONS

Figure 5 shows the distribution of effective plastic strain on each forging stage. In extrusion process, stage 1, max. plastic strain value was found around 1.2 on the shaft. In stage 2, pre-heading operation was conducted and preparation form of socket was formed. Here, max. plastic strain reached 0.5 on the head while strain values on the shaft remained the same. In stage 3, hexagonal shape was given to the head section which increases plastic strain value to 2.2. Preparation for the dog point geometry was also formed on the end of the shaft and plastic strain reached 3.6 on this area. Final geometry of the head and socket were given in stage 4. Due to the excessive forming, plastic strain was found to be around 5. On the shaft, dog- point was formed and final plastic strain value was determined as 3.9.

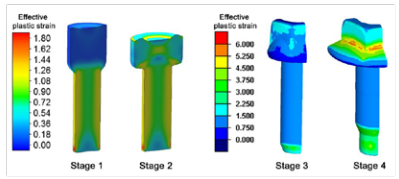

Fig. 5 Distribution of effective plastic strain on forging stages.

Contact pressure during forging of bolt head is a critical parameter to determine the critical locations on the tools during forging. For that reason, distribution of contact pressure was determined during forging as shown in Figure 6(a). After socket was completely formed, material was forced to flow through radial direction to form flange at t1 time . During the formation, punch pushes the part into tool cavity and this leads to generation of excessive contact pressure on the dog-point section. In other words, dog-point section carries high percentage of forging load alone. Naturally, this leads significant increase of tensile stress on the weakest point of the tool which is the end radius as depicted in Figure 6(b). Comparison of simulated and failed tool is shown in Figure 6(c). As seen from the figure, cracking starts from the radius and propagated through the outer diameter of the insert as a result of tensile stress. Prediction of the stress distribution was seen well matched with actual failure of the tool.

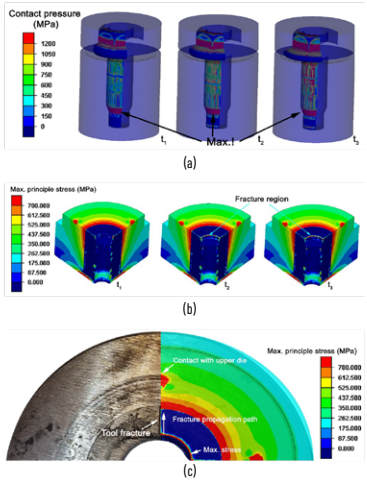

Fig. 6 a) Distribution of contact pressure at forging time of t1, t2 and t3 (t1<t2<t3), (b) max. principle stress distribution on dog-point tool (no.4) and (b) and (c) comparison of failed and simulated tool at t3.

As depicted in the above paragraph, contact pressure on the dog-point section during formation of flange and socket reached very high values, ~2500 MPa which leads crack initiation on the tool radius. To eliminate that, forging stage designs of stage 4 and 5 were changed as shown in Figure 7(a). Here, the reduction on the shaft having 26° on stage 5 was shifted to stage 4 and the dog-point formation was shifted from stage 4 to stage 5. Forming simulations were repeated with changed stage designs and lap formation was detected under the head of the part on stage 5 as shown in Figure 7(b). It was seen that material cannot flow easily through dog-point reduction area and this causes to expand of the shaft diameter under the head. Furthermore, expanded part of the shaft buckled with increasing pressure and leads to lapping. In order to ease material flow on dog- point section on the die, preparation and dog-point angle was decreased to 40° from 45°. Simulation showed that lap formation was avoided with that design chance as depicted in Figure 7(c).

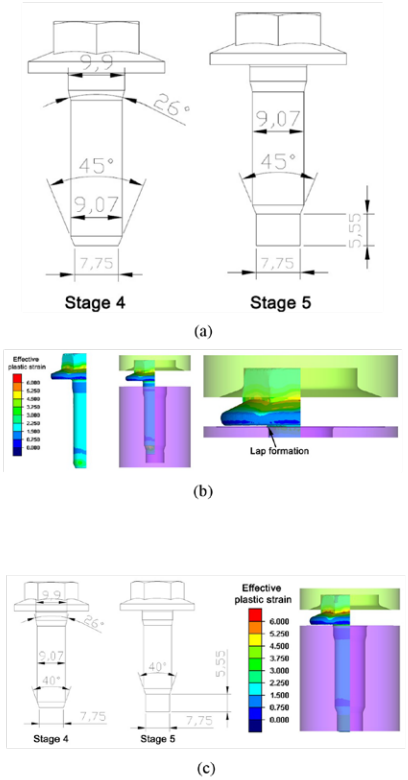

Fig. 7 (a) Design chances on stage 4 and 5, (b) lap formation on stage 5, (c) final dimensions of stage 4 and 5 and formation of the part.

According to final design of stage 4 and stage 5 which are shown in Figure 7(c), tool stress analysis of stage 5 was carried out. At first, monolithic tool design was used as shown in Figure 8(a). In metal forging operations, tools are generally designed as monolithic. When tool failure occurs on some point, the tool is split from that point in which max. stress is generated. This tool design is called split design. Simulation showed that tool failed due to stress localization on the dog-point as depicted in Figure 8(b). Max. principle stress was found to be between 750 and 820 MPa on this location. In the further analysis, tool was split from the surface upper from dog-point section at 1.9 mm as shown in Figure 9(a). This method decreased the tool stress on dog-point to 175 between 250 MPa as depicted in Figure 9(b).

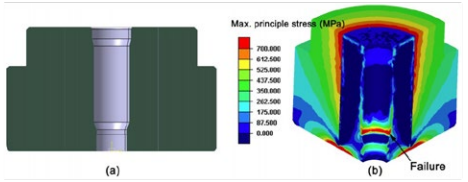

Fig. 8 (a) Monolithic design of dog-point tool and (b) max. principle stress distribution.

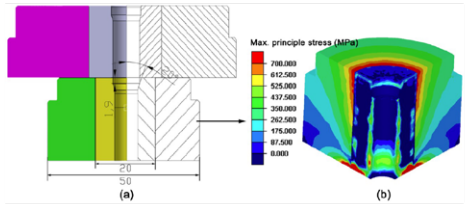

Fig. 9 (a) Split insert design of dog-point tool and (b) max. principle stress distribution.

Bolt production with new tools were performed to investigate the effectiveness of the new design on tool life. Tool life before simulations was determined as 35,174 bolts per tool for forging of 1,000,000 bolts in production house. It was seen that 28 tools were failed during that production. This production costs extremely high due to tool cost, consumed energy and inactive time of the forging press during tool change. The life of new tools are shown in Figure 10 for forging of 1,500,000 bolts. Total of 11 tools were used and tool life was determined as 136,364 bolts/tool. This showed that tool life was increased about 3.8 times.

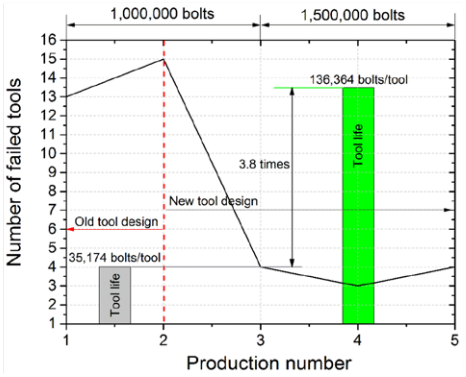

Fig. 10 Comparison of tool life of old and new tools.

5. CONCLUSIONS

In the present study, multi-stage cold forging process of special M10x32 dog-point bolts was investigated numerically to analyze the reasons of tool failure and reveal the influences of forging stage design on tool life. Simulations showed that simultaneous forming of flange, socket of and dog- point section leads to generation of excessive contact pressure and tool fracture was triggered by high tensile stress. Flow of the material on dog- point section was found to be affected by reduction angle. While 45° dog-point angle slows the flow of material and causes expansion of shaft diameter and lap formation, forming problems were vanished with reduction of this angle to 40°. It was seen that tool stress can be reduced about 70% with proper modifications on forging stage designs which leads to increase of tool life 3.8 times in production.

REFERENCES

[1] T.-W. Ku and B.-S. Kang, "Tool design for inner race cold forging with skew-type cross ball grooves," Journal of Materials Processing Technology, vol. 214, no. 8, pp. 1482-1502, 8// 2014.

[2] K. Wagner, A. Putz, and U. Engel, "Improvement of tool life in cold forging by locally optimized surfaces," Journal of Materials Processing Technology, vol. 177, no. 1-3, pp. 206-209, 2006.

[3] B. He, "Failure and Protective Measures on Punch & Die for Cold Extrusion," presented at the The 2nd International Conference on Computer Application and System Modeling, 2012.

[4] K. Andreas and M. Merklein, "Influence of Surface Integrity on the Tribological Performance of Cold Forging Tools," Procedia CIRP, vol. 13, pp. 61-66, 2014.

[5] S.-Y. Hsia and P.-Y. Shih, "Wear Improvement of Tools in the Cold Forging Process for Long Hex Flange Nuts," Materials, vol. 8, no. 10, pp. 6640-6657, 2015.

[6] P. Skov-Hansena, J. G. Niels Bayb, and P. Brùndstedd, "Fatigue in cold-forging dies: tool life analysis," Journal of Materials Processing Technology, vol. 95, pp. 40-48, 1999.

[7] S. Jhavar, C. P. Paul, and N. K. Jain, "Causes of failure and repairing options for dies and molds: A review," Engineering Failure Analysis, vol. 34, pp. 519-535, 12// 2013.

[8] H. J. Bunge, K. Pöhlandt, A. E. Tekkaya, and D. Banabic, Formability of Metallic Materials: Plastic Anisotropy, Formability Testing, Forming Limits. Berlin: Springer, 2000.

[9] M. Geiger, M. Hansel, and T. Rebhan, "Improving the fatigue resistance of cold forging tools by FE simulation and computer
aided die shape optimization," Proceedings of the Institution of Mechanical Engineers, Part B: Journal of Engineering Manufacture, vol. 206, pp. 143-150, 1992.

[10] H. Berns, A. Melander, D. Weichert, N. Asnafi, C. Broeckmann, and A. Groβ- Weege, "A new material for cold forging tools," Computational Materials Science, vol. 11, no. 3, pp. 166-180, 5// 1998.

[11] V. Vazquez, D. Hannan, and T. Altan, "Tool life in cold forging-an example of design improvement to increase service life," Journal of Materials Processing Technology, vol. 98, pp. 90-96, 2000.

[12] U. Engel and U. Popp, "Microtexturing of Cold-Forging Tools - Influence on Tool Life," Proceedings of the Institution of Mechanical Engineers, Part B: Journal of Engineering Manufacture, vol. 220, no. 1, pp. 27-33, 2006.

[13] H. C. Lee, M. A. Saroosh, J. H. Song, and Y. T. Im, "The effect of shrink fitting ratios on tool life in bolt forming processes," Journal of Materials Processing Technology, vol. 209, no. 8, pp. 3766-3775, 2009.

[14] T.-W. Ku and B.-S. Kang, "Tool design and experimental verification for multi-stage cold forging process of the outer race," International Journal of Precision Engineering and Manufacturing, vol. 15, no. 9, pp. 1995-2004, 2014.

[15] S. Yurtdaş, U. İnce, C. Kılıçaslan, and H. Yıldız, "A Case Study for Improving Tool Life In Cold Forging: Carbon Fiber Composite Reinforced Dies," Research on Engineering Structures & Materials, 2016.

[16] K. Pöhlandt, "Testing tool materials for bulk metal forming," in Materials testing for the metal forming industry: Springer, 1989, p. 176.

IMPACT OF SIMULATIONS ON COLD-FORGING DESIGNS

Cenk KILICASLAN
Tayfur YAVUZBARUT
Umut INCE

The International Journal of Forging
Business & Technology

IMPACT OF SIMULATIONS ON COLD-FORGING DESIGNS

Cenk Kılıçaslan
Tayfur Yavuzbarut
Umut Ince

Norm Cıvata San. ve Tic. A.S. (Norm Fasteners Co.); Turkey
Norm Cıvata San. ve Tic. A.Ş., 10007 Sok., A.O.S.B., Çiğli,
İzmir, Turkey

The predictive value of process and product modeling by finite-element simulations has helped in the cold forging of fasteners. In this case, the punch used in a wheel-bolt forging was reconsidered Tand redesigned to eliminate the punch "sticking" in the hollow section of the forging.

The power of finite-element simulations in our industry has increased during the last decade because of theri high predictive avility in all applied Metal-forming simulations are used to develop unique processing techniques by eliminating the high number of laboratory tests required in such research, but they are also used extensively for the predictive detection of possible material failures, forging force detection, proper die design and topology optimization in the industry.
While simulations have impact on costs, they also ease the work of people in production. For instance, increasing the service life
of dies with numerical simulation results in the office leads to a decrease in the number of die-changing operations that are done by laborers.
Compared to hot forging, material flow in cold-forging operations is less fluid. Consequently, die designing requires a lot of experience and ability to predict possible problems with the help of finite-element simulations during the design stage. This article shows that, despite the best efforts, unpredictable process failures may occur even though complete process design was coupled with finite-element simulations. Stunningly, however, the reasons for these failures again were solved with simulations that show the impact of engineering software on the forging industry.

AN UNEXPECTED PROBLEM IN WHEEL-BOLT FORGING

The cold-forging process is essential in bolt manufacturing because of the severe plastic deformation delivered to the workpiece by presses, which significantly strengthens the material without wasting any material as chips. The workpiece material is at room temperature, however, and forged material may be on the critical line of its fracture strength during deformation. Although all textbooks mention these kinds of material forging problems, failures can also be seen as a part of the whole die system. An example of this is the topic of this article.

During the production of M12x1.5x12 wheel bolts, punch failure was seen on the fourth forging stage, which caused us to increase the number of punches required to complete the specified fastener. The hexagonal shape of the bolt head is prepared on the third stage, and the final dimension of the hexagon and hollow section of the head are formed simultaneously on the fourth forging stage **(Figure 1).** Here, the punch was seen to stick in the formed hollow section, probably during the pull-out of the punch in the forging sequence, and it fractured **(Figure 2).**
The forging die system includes stationary and moving dies. The moving-die system includes a die spring that enables the deformation of the hexagonal bolt head and

the moving of the punch through the semi-bolt. At the end of the deformation, the hexagonal die and punch move concurrently in opposite directions to pull out. Here, it is crucial to understand the material flow during the process. Many metal-forming simulation software packages include forging die springs in their libraries, but the exact modeling of the spring movement is not possible. However, complex die movements can be simulated more easily by defining specific die movements as a function of time.

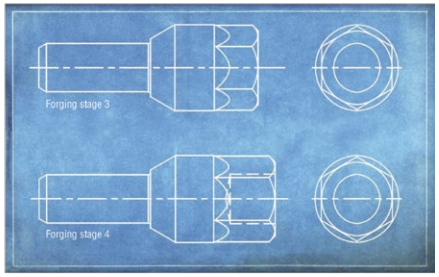

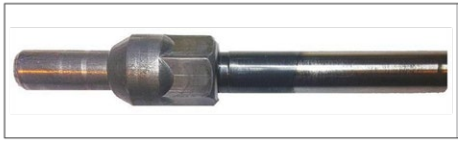

Fig. 2 Photo of failed punch

Fig. 1 Third and fourth forging stages of M12 wheel bolt

A finite-element simulation of this four- stage forging process was prepared. At first, the forming and pull-out operations on the fourth forging stage were modeled without a punch to determine the value of the decrease in hole diameter **(Figure 3).**

FINITE-ELEMENT SIMULATION: A QUICK DISCOVERY

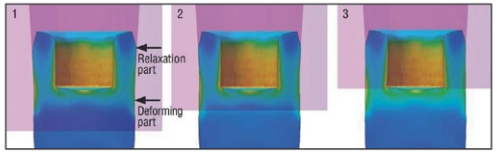

Fig. 3 Material forming during pull-out

The hexagonal die consists of a deforming part and a relaxation part. While the deforming part forges the material, the die wall was angled to decrease the friction between the flowing material and the die in the relaxation part. This allowed the material to flow more easily. It was seen that the deforming part was pushing material during pull-out, however, which led to a decrease in the diameter of the hole in the bolt on the wheel-bolt forging. As a result, the hole diameter specified to be between 11.01 and 11.05 mm was decreased to around 10.62 mm. This led to a significant increase in

the contact pressure between the punch and material.
After a critical point, the punch becomes unable to move in the cavity due to increased pressure, and it fractures as a result of high tensional stress. To eliminate that, the punch geometry was revised due to predetermined decrease on the hole diameter as depicted in ***Figure 4***. Therefore, it was predicted that the contact pressure between material and punch was decreased.

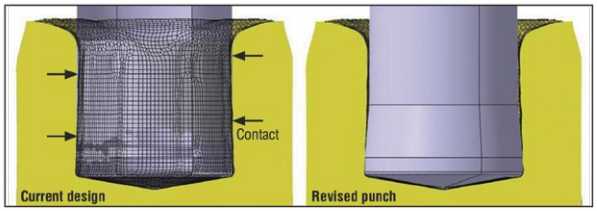

Fig. 4 Current and revised punch designs

Prove the Solution

Finite-element simulations give forging designers a chance to prove their solutions without conducting any trial-and-error tests on the shop floor. To prove a proposed solution, a new punch can be designed in generated stresses) to previous results. This methodology was performed, and the forging forces of current and revised designs were compared as shown in Figures 5a and 5b. It can be assumed that forging forces in the direction of x and y axes are responsible for the jamming of the punch in the hole of the semi-bolt. As seen Figures 5a and 5b, while revision did not alter the force history during the forming of the bolt, exerted forces on the punch were decreased during pull-out. This shows that the revised punch will not experience high pull-out loads, which leads to plastic deformation and fracture.

Thanks to advanced simulation software, it is easy to conduct stress analyses on a specified component of the die system. As we know, conducting forming simulations with elastic dies requires a lot of computational power and long CPU times. In industry, however, time is a critical variable and cannot be wasted.

In simulation software, users do not need to run 3-D simulations with elastic dies to determine stress distribution on dies and punches. Special die-load modules allow users to apply forging forces calculated from previous simulations conducted with rigid dies and apply these loads to elastic dies. In this way, CPU time is significantly decreased.
Using this module, maximum and minimum principle stress distributions on the revised punch were determined and compared to the current design as shown in

Figures 6a and 6b. Stress values were collected through a path on the circumference of the punch surface. These distributions are very important to determine the fatigue life of the punch. It can be seen that both stresses were significantly decreased with the design of a new punch.

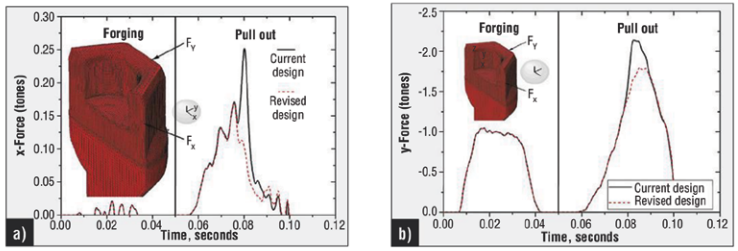

Fig. 5 Force-time curves during forging and pull-out: (a) x force, (b) y force

Conclusion

The importance and efficiency of finite-element simulations used on cold- forging applications were illustrated in this article by presenting a unique problem that occurred during wheel-bolt forging. A little time invested to prepare and run simulations eliminated a great deal of effort in labor and design, the loss of time on inactive forging presses, consumed energy and the cost of trials. Based on obtained numerical results, new punches were manufactured, and forging trials were conducted that showed the modeling results were consistent with the actual application. The wheel bolt was successfully cold forged with a single day of numerical work. Additionally, punch life was increased by a factor of four times in contrast to the previous design.

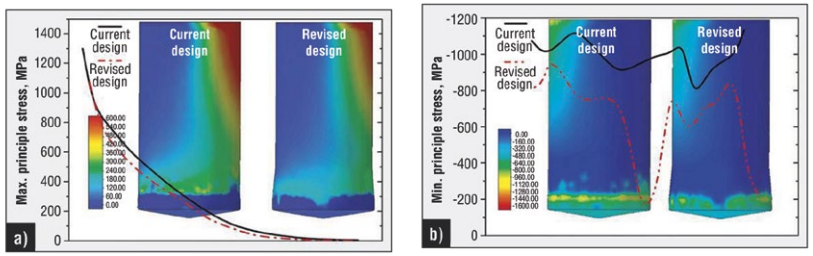

Fig. 6 Principle stress distributions on punch: (a) maximum and (b) minimum principle stresses

INCREASING COLD FORGING TOOL LIFE OF M10X1.25WELDING FLANGE NUT BY USING FINITE ELEMENT SIMULATION

Sezgin YURTDAŞ
Cenk KILIÇASLAN
N. Emrah KILINÇDEMİR
Barış TANRIKULU
Buğra KARAHAN

3. Uluslararası
Demir Çelik Sempozyumu (IISS'17)

INCREASING COLD FORGING TOOL LIFE OF M10X1.25 WELDING FLANGE NUT BY USING FINITE ELEMENT SIMULATION

Sezgin Yurtdaş*
Cenk Kılıçaslan+
N. Emrah Kılınçdemir+
Barış Tanrıkulu+
Buğra Karahan+

**Norm Cıvata San. ve Tic. A.Ş., 10007 Sok., A.O.S.B., Çiğli, İzmir, Turkey*
sezgin.yurtdas@norm-fasteners.com.tr
+ Norm Cıvata San. ve Tic. A.Ş., 10007 Sok., A.O.S.B., Çiğli, İzmir, Turkey

ABSTRACT

Cold forging of flange welding nuts requires proper design of forging stages to get tight dimensional tolerances of welding bulges and high tool life. In this study, reasons of low tool life of cold forged M10x1.25 welding flange nuts were determined by using finite element simulations and then forging stage designs were modified to decrease the tool stresses. Finite element simulations of cold forging operations were prepared in commercial finite element code Simufact. forming. Forging tests showed that two forging tools at forging stage 5 fractured due to fatigue failure during forging of 2,500 welding nuts. Numerical simulations revealed that preform of the nut before fifth forging stage was not properly formed and this led excessive increase in forging force during flow of the material in stationary tool in following forging stage. In fourth forging design, flat punch geometry was replaced by stepped punch design and closed forming case was formed on the stationary tool. It was seen that forging force in the fifth forging stage was decreased to 64 tones from 92 tones. Forging tests conducted with this design showed that tool life in fifth forging stage was increased more than 200%.

Keywords: Cold forging; nut; simulation; tool design; tool life

I. INTRODUCTION

Cold forging has a crucial role in the production of fasteners due to high mechanical properties and low material loss. Along with developing and changing technology, the use of complex fasteners is an increasing trend in the automotive, construction and aviation sectors. Complex shapes on fasteners require high forging machine capacity and tool life. These can be obtained by deep understanding of the effects of the process parameters and forging designs. Due to trial-error studies are very costly, numerical simulations become usable in metal forging process design [1]. In addition to forging station and tool designs, the effects of process parameters like tool material and surface conditions can also be investigated easily [2]. The use of CAD and CAE in the creation of new fasteners greatly shortens the product development process. Computer aided numerical simulation studies should be used to increase production and quality and reduce employment costs [3]. In the literature, many studies can be found about forging process of metals. Some of these studies were given in the followings. Geiger et al. [4] compared tool materials which were made by powder metallurgy and ceramic and their superiority against each other examined. Tools made with powder metallurgy showed compressive resistance to ~3000 MPa while ceramic materials showed higher resistance to wear. Increasing the fatigue tool life of cold forging dies is a very curial issue. In the study of Lee et al. [5], the effect of different shrink fitting ratios on die life has been investigated. It was found that the stress amplitudes plays a critical role on determining tool life and the effects of creating pre-stress and pressure to minimize the stress amplitude was clearly revealed. In a previous study of the authors [6], It was determined that the increased shrink fitting ratios between the die components increases tool life. Carbon fiber reinforced composite material was used as the stress ring material and the shrink fitting ratios between the components was increased to 3.5%. With this innovation, up to 25% die life improvements have been achieved.

In this study, low tool life of cold forged M10x1.25 welding flange nuts were determined by using finite element simulations and then forging stage designs were modified to reduce the tool stresses to increase tool life. Forging simulations and tool analyses were conducted in simufact. forming finite element software.

II. TOOL DESIGN AND FAILURE

M10x1.25 welding flange nuts were forged from annealed 20MnB4 steel alloy. Technical drawing of the product is given in Figure 1. The forging capacity of the machine used in the cold forming of this product is 300 tons. The product is forged in total of 6 stations and the station design is given in Figure 2. Billet surface has been improved in the first two stations. While station 3 is prepared for hexagonal form, flange form preparation is made at station 4. At 5th station, the final form is given before piercing and the piercing is carried out at the last station.

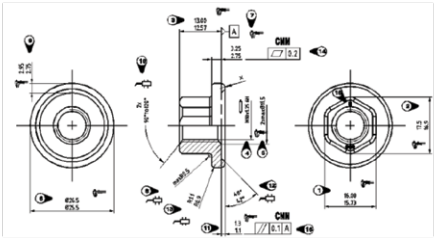

Fig. 1 Technical drawing of the M10x1.25 welding flange nut.

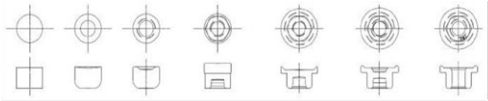

Fig. 2 Station design in production line.

2,500 numbers of the product have been cold-formed on the production line and 2 numbers of 5th station die were failed. This fracture may be formed due to ineffective preparation form in the 4th station. Technical drawing of stage 4 die couple is shown in Figure 3. While the stationary die is given on the right side, moving die is given on the left side.

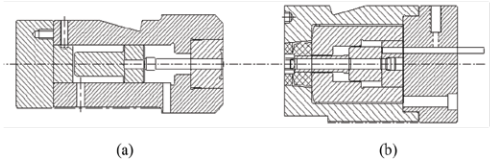

Fig. 3 Die system of stage 4; **a)** moving, **b)** stationary die.

III. NUMERICAL SIMULATIONS

Based on the station design given in Figure 2, die models were created. Numerical models of cold forging operation were prepared in Simufact.forming finite element software. Thermal effects and raw material's mechanical properties have been considered in simulations. Beside this, temperature dependent Coloumb friction coefficient was defined to the software. By this way, it was aimed to get more realistic results. Stage 1 and 2 were simulated with 2D models due to the axisymmetry while 3D models were used for stage 3, 4 and 5. As an illustration of numerical models, example of the model is shown in Figure 4. Rigid dies were used in simulations and workpiece

material, 20MnB4, was modelled as plastic material. True stress-true plastic strain curves of the workpiece between temperatures of 20 and 400 °C and strain rates between 1 and 50 s-1 were defined to the software. While in 2D models, quad elements were used in the mesh of the workpiece, in 3D models hex elements were used. In 3D models, workpiece geometry is modelled 180° and symmetry plane was determined to reduce solution time. After the forming simulations, the forming forces were determined at each station.

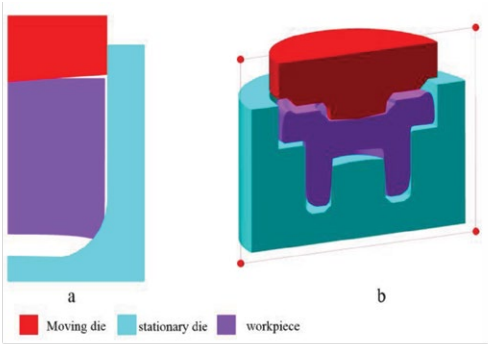

Fig. 4 Examples of numerical models; **a)** 2D axisymmetric and **b)** 3D models.

IV. RESULTS AND DISCUSSIONS

In the beginning of the study, simulations have been done to clarify the accuracy of the current design. In this respect, forging operations have been carried out according to the station designs given in Figure 2. Simulation forms in each station (ST) are given in Figure 5.

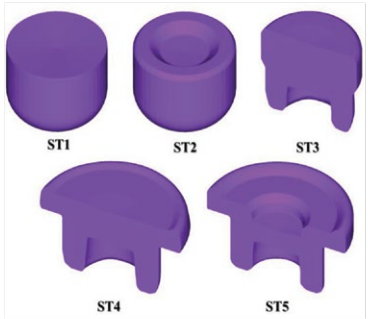

Fig. 5 Station forms obtained from simulations

Simulations revealed that welding ring form at 4th station was not properly formed. As seen in Figure 2, the height of the welding ring has to be 1.83 mm. However, the simulation showed that height of the welding ring is changing between 0.3 and 0.5 mm. Welding ring of the forged part was also measured as shown in Figure 6, and it was seen that results of simulation and forging trial are in good agreement.

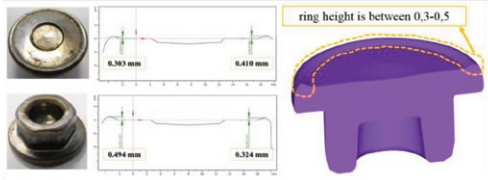

Fig. 6 Production and simulation measurement comparisons.

As followings, the forging force on 5th station was determined due to forging force has a great influence on die failure. As can be seen from the forging force graph shown in Figure 7, the forging force increased rapidly after workpiece contacted with case section of the stationary die. On each forging cycle, this high load evolution causes early breakage of the die.

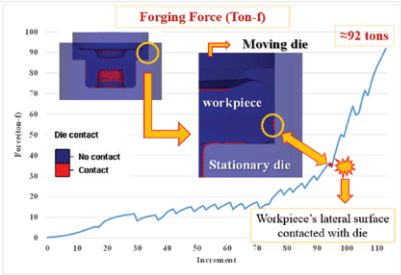

Fig. 7 Forging force versus increment graph at 5th station.

During alternative studies on the forging station design, it was aimed to make ring welding in required height by making various revisions in stationary and moving dies. In the 4th station, the case form on the moving side was replaced by the stationary side and the punch diameter was reduced from 20.2 mm to 18.5 mm as depicted in Figure 8. The revised form of stationary and moving dies were given in Figure 8.

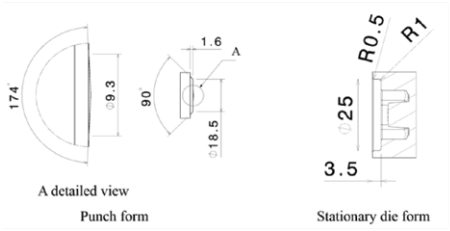

Fig. 8 Revised punch and stationary die form of 4th station.

Simulations were repeated after the design change. The ring height at the 4th station was obtained between 1.22-1.39 mm. In the current design, the forging force, which was approximately 92 tons in the 5th station, was reduced to 64 tons by the revised preparation form. Forging force experienced a decrease about 30%. The 5th station semi-finished form obtained from the simulation is shown in Figure 9. When the simulation form was checked according to Figure 1, it was determined that all the measurements were within the tolerances. In the current and revised design, difference between maximum forging force on the 5th station of current and revised design is given in Figure 10.

Fig. 9 5th station simulation form obtained from revised forging design.

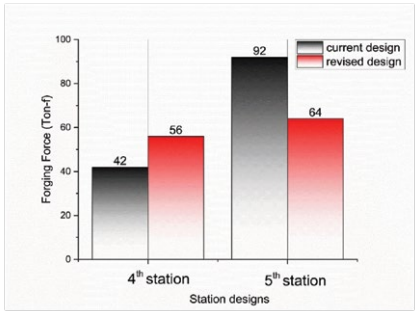

Fig. 10 Forging forces comparison between current and revised design.

Cold forging dies were manufactured according to the revised design, and forging trial was carried out. It was seen that 515,000 numbers of product have been cold-formed on the production line and only 2 numbers of 5th station die were failed. Therefore, tool life was improved more than 200%.

CONCLUSIONS

In this study, cold forged M10x1.25 welding flange nuts were investigated numerically to analyze the reasons of low cycle tool life. Simulations have been done to clarify the accuracy of the current design. The forging force on 5th station was identified due to forging force has a strong effect on die failure. The forging force during cold forging was seen to increase immediately after the workpiece contacted with case section of the stationary die. As a result of each forging cycle, this high load evolution leads early damage of the die. In the ring preparation form at 4th station, revisions were made on stationary die and punch geometry to flow of the material. In the current design, the forging force, which was roughly 92 tons in the 5th station, was decreased to 64 tons with the revised preparation form. Forging force was reduced about 30%. The forging trial was carried out and 2 numbers of 5th station die were failed when 515.000 forging cycles have been completed. It was seen that proper revisions on forging stage designs lead to increase of tool life more than 200% in production.

REFERENCES

[1] Hsia, S.-Y. and Y.-T. Chou, Fabrication Improvement of Cold Forging Hexagonal Nuts by Computational Analysis and Experiment Verification. Mathematical Problems in Engineering, 2015. 2015.

[2] Vazquez, V., D. Hannan, and T. Altan, Tool life in cold forging-an example of design improvement to increase service life. Journal of Materials Processing Technology, 2000. 98: p. 90-96.

[3] Hsia, S.-Y. and P.-Y. Shih, Wear Improvement of Tools in the Cold Forging Process for Long Hex Flange Nuts. Materials, 2015. 8(10): p. 6640-6657.

[4] Geiger, M., M. Arbak, and U. Engel, Material adapted tool design in cold forging exemplified by powder metallurgical tool steels and industrial ceramics. Production Engineering, 2008. 2(4): p. 409-415.

[5] Lee, H.C., et al., The effect of shrink fitting ratios on tool life in bolt forming processes. Journal of Materials Processing Technology, 2009. 209(8): p. 3766-3775.

[6] Yurtdaş, S., et al., A Case Study for Improving Tool Life In Cold Forging: Carbon Fiber Composite Reinforced Dies. Research on Engineering Structures & Materials, 2016.

LIGHT-WEIGHT FORGING OF STEEL ALLOY FASTENERS

Cenk KILIÇASLAN
Sezgin YURTDAŞ
Niyazi Emrah KILINÇDEMİR
Umut İNCE

International Conference
"New Developments in Forging Technology 2017"

LIGHT-WEIGHT FORGING OF STEEL ALLOY FASTENERS

Dr.-Ing. Cenk Kılıçaslan
Dipl.-Ing. Sezgin Yurtdas
Dipl.-Ing. Niyazi Emrah KılınçdemirM.Sc.
Dipl.-Ing. Umut İnce, M.Sc.

Norm Cıvata San. ve Tic. A.Ş., Turkey

ABSTRACT

Extremely growing trend in automotive industry is to decrease CO2 emissions by reducing the weight of the passenger cars while enhancing safety and integrity of automobile struc- ture. For this purpose, competition between automobile suppliers increases aggressively and research and development studies become very valuable. Light weighting e orts are mainly focused on chassis and engine components however fasteners were not deeply con- sidered for weight reduction purposes. In this study, lightweight design concepts of hex- bolts and ball studs were presented. In contrast to previous studies, weight reduction de- signs on this study do not cover the usage of non-ferrous alloys or unconventional forging techniques. Forging station designs were modi ed to get higher weight reduction ratios and cold forging process was investigated numerically by using nite element code Simufact. forming. Head of the fasteners has hemispherical hollow section for weight reduction while the rigidity was maintained. Simulations and forging trials showed that total weight of the fasteners can be reduced between 11% and 18% by using hollow head designs.

I. INTRODUCTION

Light-weight demands in automotive industry started to increase in 1970s due to high energy prices, decreasing fossil fuel sources and regulations to decrease CO emissions /1/. In last decade, emission reduction ratios were speci ed by governments and objective requires 13% reduction in CO corresponding to 182 g of CO /km until the year 2020 /2/. In addition to above mentioned environmental restrictions, light-weight designs are also required to improve economic bene ts for supplier companies to reduce material usage and cost of production energy. In automotive industry, light-weight constructions are also crucial to improve safety and driving comfort /3/. As depicted in the paper of Kleiner et al. /4/, light-weight studies include di erent types of engineering and science disciplines like mechanical designing, material science, manufacturing science and optimization me- thods. Researchers are mainly focus on developing unique methods which may include new manufacturing techniques or strengthen steels by alloying. By combining these, dif- ferent light-weight techniques can be employed to metal forming operations. In the first method (called as material based method) is on the use of high strength steels in parts while dimensions of load bearing sections are decreased. This method is e cient on weight re- duction however increase in strength of the material may cause forming problems or early tool failures. In iterative methods, material thickness is only increased on the sections of the part which are subjected to higher loads. At the rest of the part, optimized geometry is used. Detailed information about di erent methods can be found in the study of Tekkaya et al. /5/.

Although there are many studies on light-weight design and manufacturing of engine parts, chassis and powertrain, there was no investigation found in the literature about light-weight designs of cold forged fasteners. In recent years, light-weight studies were conducted to di erent types of fasteners by Norm Fasteners. Instead of using non-ferrous metals or high strength steels, cross sections of the fasteners were changed with hollow sections by maintaining the integrity. By this way, the potential of light-weight design was revealed before using non-conventional forging methods or high strength steels. In order to ful ll the gap in the literature about light-weight fasteners, lightweight designs and cold forging sequence of M14 hex-bolts (EN 1665) and Ø16 M10 ball studs were proposed in this study. Forging simulations were carried out using nite element software Simufact.forming. Ma- terial ow, distribution of plastic strains and forging forces were investigated. Simulation results were also proved by conducting forging trials.

II. LIGHT-WEIGHT DESIGN

To achieve light-weight fastener design with steel, the rst method is to use hollow geome-tries in load-free or low stressed sections instead of solid designs. M14 hex-bolts and Ø16 M10 ball studs were selected for the case study and above mentioned method was applied to these fasteners. Light-weight designs are shown in Figure 1(a) and (b) for both type of fasteners. Since the weight reduction was only applied to the head section, it is more accu- rate to compare the weight of the head of fasteners by neglecting shafts. With this conside- ration, weight reduction is about 11% for the bolt and 18% for the ball stud.

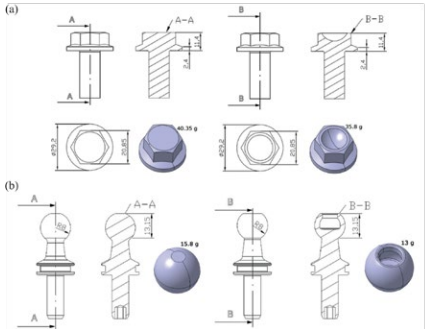

Fig. 1 Original and light-weight designs of (a) M14 hex-bolts, and (b) Ø16 M10 ball

III. NUMERICAL MODELS OF LIGHT-WEIGHT FORGING

Numerical models of each forging station of both fasteners were prepared in Simufact.for- ming nite element software. Forging simulations were carried out using coupled thermo- mechanical analysis method. Figure 2 shows the examples of models. Numerical models consisted of moving and stationary dies and work-piece. Moving die was attached to the de ned press and stationary die was constrained in all directions and rotations. Both dies were modeled as rigid. Work-piece was modeled as plastic material and elastic deforma- tions were ignored because elastic deformations have negligible e ects on the deformation of the material in a pure bulk forming operation like forging. Flow curves of work piece material at varying strain rates and temperatures were de ned to the software. As shown in the gure, axisymmetric parts were modeled in 2D (Figure 2(a)) while others were mo- deled in 3D (Figure 2(b)). The FE mesh distributions of work-piece in 2D and 3D models are also shown in Figure 2(a) and (b), respectively. In 2D simulations approximately 3,000 numbers of quad-elements were used while 40,000 numbers of hexahedral elements were defined for parts in 3D simulations. In contact de nition, temperature dependent Coulomb friction model was used.

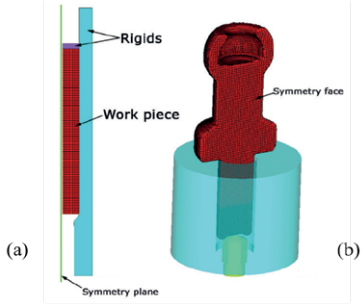

Fig. 2 Examples of numerical models; (a) 2D and (b) 3D models

IV. RESULTS

E ective plastic strain distribution on the M14 bolt after cold forging shown in Figure 3(a). As depicted in the gure, no severe and localized deformation was observed on the hollow sections that may cause failure of the parts. Semi-spherical shape was given to the head section of M14 bolts between initial and last forging stations. Here, the depth of hollow section is critical to obtain a ordable forging forces. As shown in Figure 3(b), an initial shape of the hex was given to the hollow headed semi-bolt. During forming, diameter of the hollow section decreased and the geometry changed its form from semi-spherical to ellipse. This phenomenon has to be carefully investigated by numerical simulations and proper initial diameter should be selected not to e ect the nal forming process as shown in Figure 3(b). If the decrease in diameter is not controlled carefully, forming failures like lapping will be seen on the product.

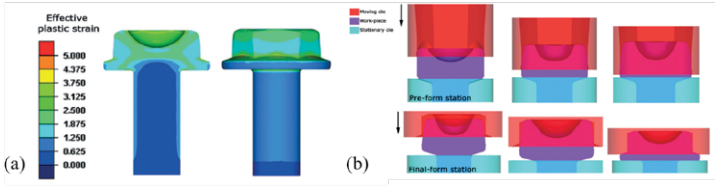

Fig. 3 (a) E ective plastic strain distribution on M14 hex-bolt and (b) preparation for forming hex-heading and (b) nal forging station of hex-head

During light-weight forging of ball stud, spherical head form was given by bending of the hollow section using proper punch geometry. On the other hand, improper bending may cause high residual stresses that may cause damage in the product. It was seen that e ective plastic strain values on the area depicted with arrows are between 3 and 4 due to bending of hollow section into spherical geometry while the rest area experienced plastic strain values around 2 as seen in Figure 4. This showed that forming limits were excessi- vely not exceeded.

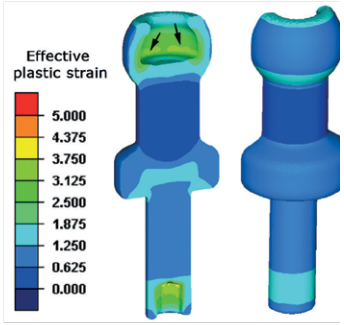

Fig.4 Distribution of e ective plastic strain on Ø16 M10 ball stud

Figure 5(a) and (b) shows the forging force-stoke curves of each forging station of M14 bolt and Ø16 M10 ball stud. Total forging forces are 181 and 137 tons for the bolt and ball stud, respectively. According to previous investigations, total forging force was seen to increase in M14 bolts due to spherical shaped cavity on the head in contrast to its solid design. However, hollow head usage in ball stud signi cantly decreased the total forging force due to decrease in mass of the part that is formed.

M10 ball stud

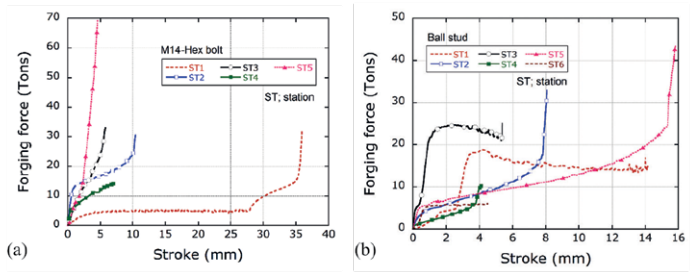

Fig. 5 Forging force versus stroke curves of each forging station; (a) M14 hex-bolt and (b) Ø16 M10 ball stud

Light-weight forging of hex-bolt and ball stud were conducted in Norm Fasteners and the pictures of the products are shown in Figure 6. As depicted in the picture, fasteners were well formed without any failure. For each fastener, at least 200,000 parts were forged and no tool failure was observed.

Fig. 6 Pictures of light-weight forged (a) bolt and (b) ball stud

V. CONCLUSIONS

In this study, lightweight designs of steel alloy hex-bolts and ball studs were presented. In contrast to work being done by many researchers and engineers, light-weight designs of these fasteners do not cover the usage of non-ferrous alloys or unconventional forging techniques in

this work. Weight of the head of the fasteners was reduced between 11% and 18%. Finite element simulations showed that hollow headed fasteners can be cold forged successfully by modifying the forging stations. The study also proved that conven- tional engineering techniques should be applied rst to current designs to achieve light- weight cold forged products before using non-ferrous alloys or unconventional forming techniques.

LITERATURE

/1/ Osakada, K. — Cold Forging in Japan, Presentation at the 40th International Cold Forging Group, Plenary Meeting, Padova, Italy, September, 2007.

/2/ Tekkaya, E. et. Al. — History and Future of Cold Forging in Europe, Presentation at the 40th International Cold Forging Group, Plenary Meeting, Padova, Italy, September, 2007.

/3/ Lange, K. Cser, L. Geiger, M. Kals, J.A.G. — Tool Life and Tool Quality in Bulk Metal Forming. CIRP Annals 41 (1992) 2, 667-675.

/4/ Groenbaeck, J. Hinsel, C. — Improved Fatigue Life and Accuracy of Precision Forging Dies by Advanced Stripwound Prestressing System, SME Clinic on Precision Forging Technology, Columbius, Ohio, USA, Nov. 10, 2000.

/5/ Groenbaeck, J. Hinsel, C. — Optimization of Tool Life & Performance Through Advanced Material and Prestress Design, NACFG Conference, Columbus, Ohio, USA, September, 2003.

/6/ Brecher, C. Schapp, L. Tannert, M. — Simulation-aided optimization of multistage dies – Coupled simulation of forging processes with non-linear-elastic machine models. In: Denkena, B. (edtr.): Proc. 1st Int. Conf. on Process Machine Interactions PMI, Hannover, Germany, 2008, pp 167-174.

/7/ Engel, U. Geiger, M. Kroiss, T. Völkl, R. — Process-machine interactions in cold forging – calculation of press / tooling sti ness and its integration into FE process simulation. In: Yang, D.Y. (edtr.): Proc. of the 9th International Conference on Technology of Plasticity (ICTP), Gyeongju, Korea, 2008, pp 1735-1740.

MANUFACTURING WITH MICRO-ALLOYED STEELS: ECONOMICALLY & ECOLOGICALLY

Tayfur YAVUZBARUT
Emrah KILINÇDEMİR
Barış TANRIKULU
Fatih Cemal CAN

Fastener Technology International

MANUFACTURING WITH MICRO-ALLOYED STEELS: ECONOMICALLY & ECOLOGICALLY

Tayfur Yavuzbarut
Emrah Kılınçdemir
Barış Tanrıkulu

Norm Civata San. ve Tic. A.Ş.,
Turkey (Norm Fasteners)
Fatih Cemal Can
İzmir Katip Çelebi University, Department of Mechatronics Engineering

Bolts are the main fastener parts of machine assembly in the automotive, machine, robot and vehicle industries. An assembly process without bolts is possible, but it is very rare in recent production technology. Therefore, bolts have been very important machine elements since the beginning of the first industrial revolution.
Bolts are formed by cold forging manufacturing technol- ogy in mass production. There are several stages to form a bolt according to standard dimensions and grades. Cold forg- ing provides the forming of material by pressing it between moving and stationary dies at ambient temperature. Before the cold forging operation, spheroid annealing is applied to conventional materials for wire rod (raw material) to impart to the material a homogeneous and softer microstructure. This annealing process consists of heating, holding on high temperature and the cooling sections. Annealing temperatures range from 700°C to 750°C, and the total duration of this operation is 26 hours.

The raw materials, which are obtained from supplier com- panies, are annealed and then surface treatment is applied. The purpose of surface treatment is to decrease the coefficient of friction between the workpiece and the tooling by covering the wire rod with a phosphate layer. The dies used in the production of fasteners are composed of carbide insert materials being pressed-fitted into air steel (H13). There are many factors that affect tool life. Die ge- ometry, the surface quality of the billet, forging forces, tool production, design and human effects are direct factors having an influence on die life.
The fasteners used in the automotive industry are required to have high stability due to the critical locations in which they are used. Therefore, one of the most important factors in the part design is having the high strength feature. There are a lot of mechanical properties, which consist of hardness and strength values, based on ISO 898-1 "Mechanical properties of fasteners made of carbon steel and alloy steel–Part 1: Bolts, screws and studs with specified property classes–Coarse thread and fine pitch thread". Conventional raw materials used in the production of fasteners have to be heat treated for chang- ing microstructure and improving their mechanical features that are required by the OEM after the cold forging process. However, heat treatment is a process that is costly, extends process steps and has adverse affects on the workpiece surface.
New-generation materials are produced with rapidly im proving material technologies. It is possible to obtain different strength values with micro-alloyed steel materials with high strength properties by forging. The use of micro-alloyed steels and unique station designs in the production of the long ball stud and M8 DIN 933 with grade 8.8 have allowed proper manufacture through cold forging with no heat treatment

(Figure 1).

Fig. 1 Long ball stud and M8 DIN 933 bolt.

In this study, manufacturing simulations are carried out by using numerical simulation techniques in order to capture the probable die defects, determining the process parameters such as press forces and die stresses as well as predicting the tool life, residual stresses, material flow and forecasting the mechanical properties occurred after forging previous to project initiation. In conclusion, it is seen that the results exported from the numerical analysis and the experimental results are vastly consistent with each other. Hence, the use of micro-alloyed steels in the cold forging process has the ability to eliminate the subsequent heat treatment process that results in significant advantages both economically and ecologically.

MATERIALS FOR BOLTS

The materials, which are mostly preferred for cold forging, are listed in **Table 1.** Steels with low or medium carbon are generally used for cold forging manufacturing. These materials need heat treatment before the cold forg- ing operation because the materials must have a spherical homogeneous microstructure.

Table 1. Conventional Raw Material.

Malzeme	C %	Si %	Mn%	P < %	Cr %	Mo %
QSt. 36-3	0.06-0.13	<0.10	0.25-0.45	0.040	-	-
20MnB4	0.17-0.23	0.15-0.35	0.8-1.0	0.035	-	-
C 25	0.22-0.29	< 0.40	0.40-0.70	0.045	< 0.40	< 0.10
32Cr4	0.30-0.35	0.10-0.40	0.60-0.90	0.035	0.90-1.20	-

Micro-alloyed steels, 27MnSiVS6, 35V1 and S550MC are used to eliminate heat treatment in this study.

DESIGN AND SIMULATION

In this article, we describe an attempt to manufacture M8x30 DIN933 bolts without heat treatment. The particular station design of cold forging is shown in **Figure 1.** The billet of the bolt is formed to a bolt shape through four stages as illustrated in **Figure 2.**
Die assembly drawings of four stations can be seen in **Figure 3.** The extrusion process is realized in the first station. Then, upsetting is performed in the second station. The third stage is related to the chamfered end process. The cutting operation is in the final stage.

The simulation studies were carried out according to die design for the M8x30 DIN933 bolt. Computer-aided mod- eling of the process is shown in **Figure 4.** The simulation was run until the third station. Material flow curves, which were used in the simulation studies, are determined in room temperature and by using devices in the **NORM Research.**

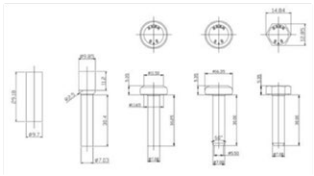

Fig. 2 Stage design for M8x30 DIN 933 bolt.

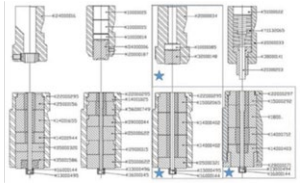

Fig. 3 M8x30 DIN 933 bolt mold assembly drawing.

Fig. 4 Modeling for M8x30 DIN 933 bolt. drawing.

DEVELOPMENT CENTER

Plastic strain distribution of the stages that was obtained from simulation result is shown in **Figure 5.**

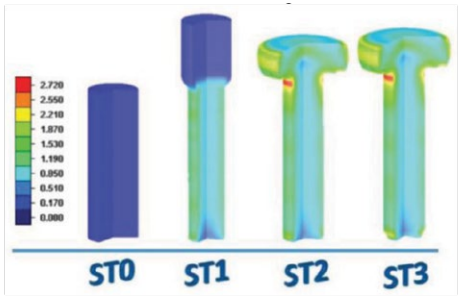

Fig. 5 Equivalent plastic strain distribution.

There is a relationship between the Vickers hardness number (HV) and the flow stress (Y) of the material. In cold forming practice, this relationship has to be used in the fol- lowing manner:

1. Obtain the flow curve of the workpiece material up to high plastic strains as accurate as possible.
2. Adapt this curve into the simulation software.
3. Create a model with true boundary conditions as accurate as possible and run the simulation.

4. Determine the flow stress value (MPa) corresponding to the equivalent plastic strain point you wanted.
Formulations for expected hardness are represented as follows:
Tabor: HVx9.81=2.9xY (1) Tekkaya: HVx9.81=2.475xY (2) Tekkaya&Yavuz: HVx9.81=2.527xY (3)
Using these formulations, the hardness of the bolt was ex- pected as shown in Figure 6. According to Tabor formulation, hardness values were found to be suitable for desired hardness.

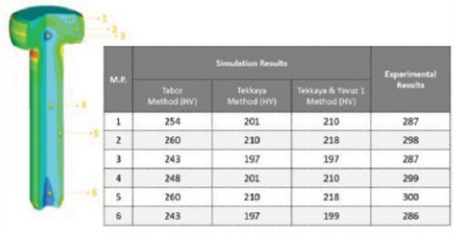

M.P.	Simulation Results			Experimental Results
	Tabor Method (HV)	Tekkaya Method (HV)	Tekkaya & Yavuz 1 Method (HV)	
1	254	201	210	287
2	260	210	218	298
3	243	197	197	287
4	248	201	210	299
5	260	210	218	300
6	243	197	199	286

Fig. 6 Hardness expectation and experimental results.

According to ISO 898-1, the range of hardness through the shaft and head has to be from 250 HV to 320 HV. It was seen that hardness values of the parts that have been produced were suitable. Another requirement of this standard for 8.8 property class is minimum 800 MPa tensile and 640 MPa yield strength. The tension test results of the real specimens have been illustrated in **Figure 7.**

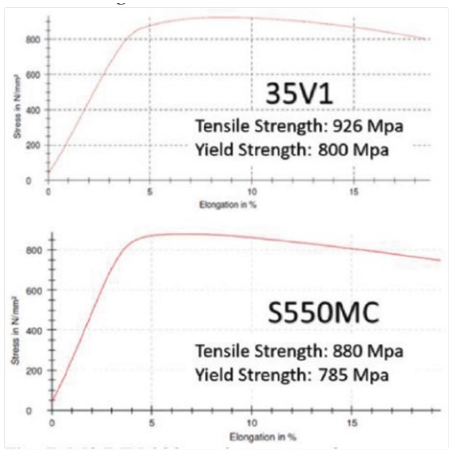

Fig. 7 M8 DIN 933 tesnion test results.

CONCLUSIONS

he new micro-alloy steel materials (35V1 and S550MC for M8x30 DIN 933 bolt) and (27MnSiVS6 for long ball stud) were manufactured in this study. Only bolt results were shared. The results of this study are as follows:

• All manufactured parts meet all requirements according to ISO 898-1.

• By using the unique station design in production with micro-alloyed materials, it is possible to eliminate annealing and heat treatment processes.

• Production steps and CO2 emissions have been reduced and ecological production has been achieved.

• 35V1 and S550MC have similar results and can be used interchangeably.

• Tabor hardness expectation method and experimental results are similar.

• Precisely determining the flow curves is very important for obtaining the right results.

www.normcivata.com / www.normgroup.com.tr

EXPERIMENTAL INVESTIGATION ON SELF-LOOSENING OF PRELOADED STAINLESS STEEL FASTENERS

Umut İNCE
Barış TANRIKULU
N. Emrah KILINÇDEMİR
Sezgin YURTDAŞ
Cenk KILIÇASLAN

3. Uluslararası
Demir Çelik Sempozyumu (IISS'17)

EXPERIMENTAL INVESTIGATION ON SELF-LOOSENING OF PRELOADED STAINLESS STEEL FASTENERS

Umut Ince*
Barış Tanrıkulu+
N. Emrah Kılınçdemir+
Sezgin Yurtdaş*,
Cenk Kılıçaslan+

**Norm Cıvata San. ve Tic. A.Ş., 10007 Sok., A.O.S.B., Çiğli, İzmir, Turkey*
+ Norm Cıvata San. ve Tic. A.Ş., 10007 Sok., A.O.S.B., Çiğli, İzmir, Turkey

ABSTRACT

Use of stainless steel bolts has become widespread due to their high resistance to corrosive environment. However, the widespread use of stainless steel bolts brought together many unknowns in assembly conditions. In particular, there are not many studies present in the literature that concerning the behaviour of stainless steel fasteners under transverse vibration conditions. Within the scope of our work, Junker vibration tests were carried out on M12x1.75x40 A2-70 bolts with a combination of axisymmetric nut, double nut and prevailing nuts which all have a locking mechanism. Then, the vibration loosening rates were compared. In addition, Torque-Clamp load tests on existing bolts were performed to obtain friction coefficients and torque-clamp load graphics. The result of the study shows that stainless bolts and nuts with different mechanical locking mechanisms behave differently under vibrational conditions.

Keywords: Stainless steel; Fastener; Vibration; Loosening; Friction coef.

I. INTRODUCTION

Stainless steel fasteners have a huge range of application area in the industry, especially where the corrosive atmospheres are dominant. Stainless steel fasteners differ in mechanical behaviour from conventional bolts. Exposure of the bolts to vibration which results severe loss of clamp load causing undesired problems. The most frequently encountered problems in fastener industry were the loosening due to vibration because of insufficient clamp loads and breakage due to over torqueing. For this reason, it is necessary to determine as much as possible the torque value at desired clamp load before the assembly operation. Inspection of transvers vibration effects on fasteners has begun with Junker et al. [1]. According to Junker, vibration in transvers direction has a critical role in loosening process. Researches on vibration have continued and it was found that friction coefficient has a key role in loosening processes [2]. Many other studies based on the transvers vibration has been conducted with different combinations of fastener-nut- washers to determine the effects of these on loosening. [3–8]. Researchers mainly focused on finding a mathematical model for describing the behaviour of loosening processes. Nassar and Yang [9], generated a mathematical model which is used for predicting the preload loss in a vibrational condition.In this study, Junker vibration tests were carried out on M12x1.75x40 A2-70 bolts with a combination of axisymmetric nut, double nut and prevailing nuts which all have a locking mechanism. Then, the vibration loosening rates were compared.

II. EXPERIMENTAL TEST PROCEDURE

In the study three different type of stainless steel nuts, double nut, axisymmetric nut and prevailing nuts, were used. These nuts were mainly used in the industry for providing better loosening solutions in corrosive environment. In the first part of the study, torque tension test were conducted for determining the friction coefficient and preload value for 30 Nm torque. The pictures of each specimen is given in Figure 1. During the tests, only one specimen was used for each test to eliminate the effects of friction coefficient increase after one use. Bolts used for the tests were classified as M12x1.75x40 A2-70 stainless steel bolts.

In the study three different type of stainless steel nuts, double nut, axisymmetric nut and prevailing nuts, were used. These nuts were mainly used in the industry for providing better loosening solutions in corrosive environment. In the first part of the study, torque tension test were conducted for determining the friction coefficient and preload value for 30 Nm torque. The pictures of each specimen is given in Figure 1. During the tests, only one specimen was used for each test to eliminate the effects of friction coefficient increase after one use. Bolts used for the tests were classified as M12x1.75x40 A2-70 stainless steel bolts.

Fig. 1 M12 x 1.75 x 40 A2-70 fasteners with double nut, axisymmetric nut and prevailing nut

Friction coefficient values were calculated based on the preload value which has been measured during torque-tension tests according to EN ISO 16047:2005, which was given in
Equation 1;

$$\mu_{total} = \frac{T/F - P/2\pi}{0{,}577 d_2 + 0{,}5 d_b}$$

In the study three different type of stainless steel nuts, double nut, axisymmetric nut and prevailing nuts, were used. These nuts were mainly used in the industry for providing better loosening solutions in corrosive environment. In the first part of the study, torque tension test were conducted for determining the friction coefficient and preload value for 30 Nm torque. The pictures of each specimen is given in Figure 1. During the tests, only one specimen was used for each test to eliminate the effects of friction coefficient increase after one use. Bolts used for the tests were classified as M12x1.75x40 A2-70 stainless steel bolts.

III. RESULTS AND DISCUSSIONS

Torque-tension test for double nuts were conducted with 2 step torqueing. Firstly, smaller nut which was called as “1.Nut” was torqued at a value of 12 Nm which was the %40 of the desired torque. Secondly, the ticker nut which is called as “2. Nut” was torqued at a value of 30 Nm. The result of the double nut torque tension test was given in
Figure 2.

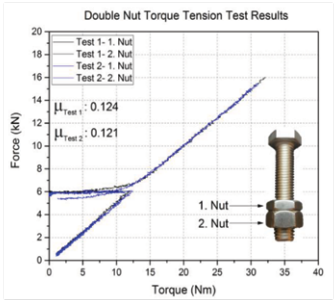

Fig. 2 Double nut torque-tension test results.

According to the test results, friction coefficient was found around 0.12 which was an ideal value for bolts. It was also found that 30 Nm torqueing value gives 16 kN clamp load on the fastener. Clamp load values which was then used in the junker vibration test for the starting point. Torque tension test of axisymmetric nuts were also conducted with 2 times torqueing. Test result for the axisymmetric nut tests were given in
Figure 3.

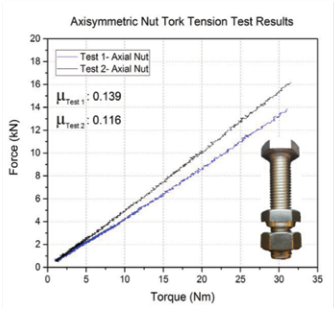

Fig. 3 Axisymmetric Nut torque-tension test results.

According to the test result, it is clearly seen that the clamp load value for 30 Nm was approximately same with the double nut value. Desired clamp load at a same torque value can be only changed by adjusting the friction coefficient in these conditions. The last torque tension were conducted with prevailing nut. The result for prevailing nuts were given in
Figure 4.

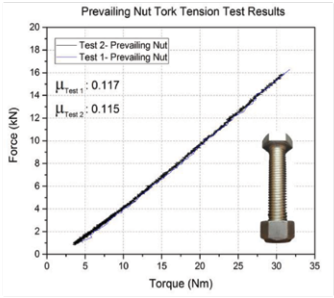

Fig. 4 Double nut torque-tension test results.

Result for the prevailing nut torque tension test showed that the friction coefficient value for all three type nut was between 0.11-0.13 and the clamp force values were between 14-16 kN. For the junker vibration test 15 kN clamp load forces was used as the starting references for all three type of nuts. Junker tests were conducted with 0.9 mm relative displacement at 3 Hz in transverse direction. The preload loss was measured during the test and results were graphically shown in a preload loss-cycle plot. Five tests were conducted for each nut type and the average values were taken. Test results for double nuts were given in
Figure 5.

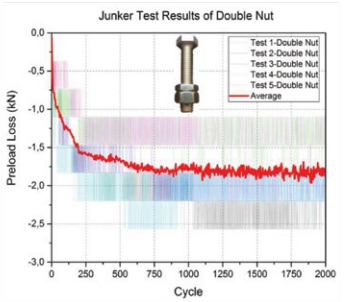

Fig. 5 Double nut Junker vibration test results.

Result of the junker vibration test of double nuts shows that there has been a very sharp preload loss in the first 250 cycle of the test which was seen around 1.6 kN. The lost in 2,000 cycle which is considered as the limit of loosening cycle in junker vibration test was around 2 kN.

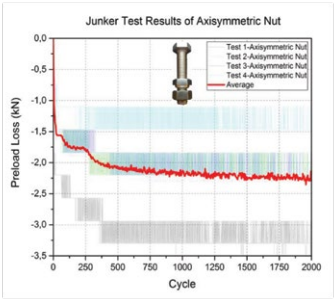

Fig. 6 axisymmetric nut Junker vibration test results.

The result of the axisymmetric nut on junker vibration test given in Figure 6 shows that sudden preload loss also happened in the first 250 cycle with a value of 1.8 kN. The total loss for the nut in 2,000 cycle was around 2.2 kN.

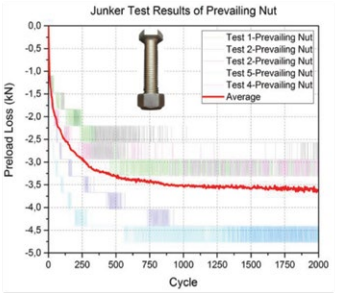

Fig. 7 Prevailing nut Junker vibration test results.

From the test result given in Figure 7, it is clearly seen that the preload loss at the first 250 cycle was around 3 kN. The total loss was approximately 3.5 kN for 2,000 cycle. For understanding the loosening behaviour of both nuts, preload loss averages have been comparatively drawn in the same plot which was given in
Figure 8.

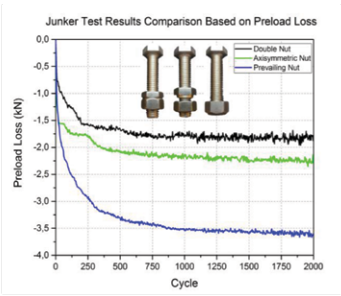

Fig. 8 Junker vibration test preload loss comparison

According to the comparative test results, it was clearly seen that prevailing nut showed the highest loss in preload loss during the junker vibration test in contrast to rest of the nuts. It can be also seen that sudden drop in preload during the test continues up to 500 cycle. As a result of that, it can be concluded that fasteners which has a double nut or axisymmetric nut have higher resistance to vibration loosening.

CONCLUSIONS

In this study, vibration loosening performances of stainless steel double nut, axisymmetric nut and prevailing nuts were investigated experimentally and comparative test results based on the preload loss has been given. Torque-tension tests were showed that friction coefficient for all three type bolt-nut combination has approximately the same, ~0.12. Clamp load was found as 16 kN in average for torque value of 30 Nm. Junker vibration tests were showed that all nuts except prevailing nut showed sudden drop in preload during the first 250 cycle of the tests. It was found that prevailing nut has the highest drop in clamp force of 3.5 kN in contrast to double and axisymmetric nuts which were experienced 2 kN and 2.2 kN loss in clamp force, respectively. Experimental study conducted on stainless steel M12x1.75x40 A2-70 bolts and nuts had clearly showed that double nut has the higher vibration resistance among others.

REFERENCES

[1] G.H. Junker, New Criteria for Self-Loosening of Fasteners Under Vibration, SAE Trans. 78 (1969) 314–335. doi:10.4271/690055.

[2] T. Hattori, M. Yamashita, H. Mizuno, Loosening and Sliding Behaviour of Bolt-Nut Fastener under Transverse Loading, in: EPJ Web ofConferences 6, 2010. doi:10.1051/epjconf/20100608002.

[3] P. Gutowski, M. Leus, Tribology International The effect of longitudinal tangential vibrations on friction and driving forces in sliding motion, Tribol. Int. 55 (2012) 108–118. doi:10.1016/j.triboint.2012.05.023.

[4] G.E. Ramey, Experimental Analysis of Thread Movement in Bolted Connections Due to Vibrations, Res. Proj. NAS8-39131, Auburn Univ. (1995).

[5] B.A. Housari, S.A. Nassar, Effect of Thread and Bearing Friction Coefficients on the Vibration-Induced Loosening of Threaded Fasteners, 129 (2014). doi:10.1115/1.2748473.

[6] M. Holland, D. Tran, Effects of Vibration on a Coulomb Friction System, Sch. ACME, Victoria Univ. (2007).

[7] D.P.Hess, O.P.Keifer, C.B. Moody, Tests on Loosening of Aviation Threaded Fasteners with Different Washer Configurations, J. Fail. Anal. Prev. 14 (2014) 683–689. doi:10.1007/s11668-014-9873-8.

[8] T. Yokoyama, M. Olsson, S. Izumi, S. Sakai, Investigation into the self-loosening behavior of bolted joint subjected to rotational loading, Eng. Fail. Anal. 23 (2012) 35–43. doi:10.1016/j.engfailanal.2012.01.010.

[9] S.A. Nassar, A Mathematical Model for Vibration-Induced Loosening of Preloaded Threaded Fasteners, 131 (2009) 1–13. doi:10.1115/1.2981165.

ON THE COLD FORGING OF 6082 H13 AND T4 ALUMINUM ALLOY BUSHES

Buğra KARAHAN
Umut İNCE
Sezgin YURTDAŞ
N. Emrah KILINÇDEMİR
Fuat Can AĞARER
Cenk KILIÇASLAN

5th International Symposium on
Innovative Technologies in Engineering and Science (ISITES2017)

ON THE COLD FORGING OF 6082 H13 AND T4 ALUMINUM ALLOY BUSHES

[1]Buğra Karahan
[1]Umut İnce
[1]Sezgin Yurtdaş
[1]N. Emrah Kılınçdemir,
[2]Fuat Can Ağarer
***[1]Cenk Kılıçaslan**

[1]Norm Cıvata San. ve Tic. A.Ş., A.O.S.B., İzmir, Turkey
[2]Norm Somun San. ve Tic. A.Ş., A.O.S.B., İzmir, Turkey

ABSTRACT

In this study, manufacturability of Ø23x36 aluminum bushes with EN AW 6082-AlSi1MgMn aluminum alloy was investigated. Two different pretreated EN AW 6082 alloys, H13 (strain-hardened) and T4 (solution annealing and naturally aged) were used in the present study and cold forging performance of the alloys was evaluated comparatively. Compression tests were carried out at different temperatures and strain rates to model the flow stress of the alloys. Extrusion tests were carried out on Zwick test machine in order to determine the material flow and sticking behavior. Cold forging trials were performed on a press having 300 tones capacity in Norm Fasteners. All experiments and forging operation were also coupled with finite element (FE) simulations by using Simufact.forming commercial software. Extrusions tests showed that the level of sticking phenomenon on dies are high for T4 alloy in contrast to H13 alloy. Cold forging trial showed that both alloys can be forged into desired shape without experiencing any failure. It was seen that surface roughness parameter of the cold forged T4 and H13 bushes was 3.81 µm and 0.99 µm, respectively. Numerical and experimental compression force-displacement curves were also found to be in good agreement.

Keywords: Aluminum, EN AW 6082, cold forging, simulation.

I. INTRODUCTION

Cold forging is an extremely important and economical way for designers to create automotive components with high production rates and good mechanical strength. As a result of the developments in forging technology, complex parts such as non-standard bolts and nuts, ball joints and gears can be formed with better mechanical properties and geometrical accuracy [1-2]. Some of the advantages provided by this process include: (a) high production rates, (b) excellent dimensional tolerances and surface quality of forged parts, (c) significant savings in material in contrast to machining, (d) high tensile strength at the forged part, (e) suitable grain flow for higher strength [3].

In modern transportation sector, using the lightweight components is necessary due to economic and environmental restrictions.In the last decade, emission reduction ratios have been determined by governments. This ratio is aimed to be reduced to 95 g CO2 / km with a 27% reduction by 2020 under the EU Regulation No 443/2009 [4]. In addition, lightweight structures used in the automotive industry are important for enhancing safety and driving comfort [5]. Weight reductionstrategies are classified into four main categories as: material lightweight design, component lightweight design, functional lightweight design and conditional lightweight design [6].

The reduction in vehicle weight is mainly related to the use of lightweight materials such as aluminum alloys [7-8]. Aluminum alloys exhibit an attractive combination not only for a long service life but also low density, high specific strength, formability and excellent corrosion resistance, but also an important requirement for recycling [9-10)]. 6xxx alloys within this group have been extensively studied due to technical considerations and reliable strength can be obtained by precipitation hardening. 6xxx series are also widely used for automotive and aerospace components due to their impact on weight reduction [11]. The 6082 alloy in this group is predominant due to its combination of higher mechanical properties, excellent corrosion resistance, convenience for T6 aging, and good weldability when compared to 6xxx alloys [12- 13].

Although aluminum alloys exhibit nearly equivalent stiffness and two times higher specific strength compared to steel, they are disadvantageous in terms of raw material cost. Therefore, it is necessary to reduce the waste material and reduce the number of defective parts by using process optimization due to high raw material cost of aluminum [14]. Anjabin and Taheri [15] investigated the effect of different aging parameters on the mechanical properties of the 6082 alloy in their work. Flow curves were determined with uni-axial tensile tests at room temperature and material model was constituted. In addition, the force-displacement curves were analyzed and the experimental data and the model were compared. To verify the results which were predicted by the model, uni-axial compression was conducted using Abaqus software. Experiment and simulation results showed that the flow behavior of 6082 alloy is divided into two groups for underage condition and overage condition. According to this, flow stress increased and the uniform elongation decreased with increasing the aging temperature or aging time in underage condition. In contrast, increase in aging time and temperature leads to decrease in flow stress and increase in uniform elongation. Wang et al. [16] investigated the hot deformation behavior of 6082 alloy. True stress-true strain curves are obtained by performing compression tests at different temperatures (425 °C, 450 °C, 475 °C, 500 °C) and strain rates (0.01 s^{-1}, 0.1 s^{-1}, 1 s^{-1}, 10 s^{-1}). According to results, flow stress was found to increase with increasing strain rate and decreasing deformation temperature. The optimum hot working condition for 6082 aluminum alloy at the strain of 0.4 was found to be 470-490 °C and 0.1-0.3 s^{-1} as strain rate. Ishikawa et al. [14] investigated the effects of thermal pulls on cold forged aluminum parts. As a result of the high thermal conductivity of aluminum compared to other metals, the thermal geometry changes in aluminum alloys have been pointed out. In the study, FE analysis was carried out using Simufact.forming software. These analyzes have shown that non- uniform temperature distributions cause local heat shrinkage on the part. Cylindrical compression tests were carried out to simulate flow curves of EN AW 6061 alloy and simulations have been conducted. Bay et al. [17] calculated friction stress for aluminum 6082 alloy, steel, and stainless steel by adopting a tribology testing system that can be simulated at different pressures, reduction ratios, surface propagation, sliding dies, and die-to-work interface temperatures. FE and laboratory test results were analyzed and evaluated together. The results showed that the pressure and interface temperature between the die-workpiece were significantly more effective than other factors. Dubar et al. [18] investigated the effect of MoS2 lubricant on sticking behavior of aluminum 6082 alloy during cold forging. In this study, FE simulations and experimental studies were evaluated comparatively. According to results, MoS2 lubricant reduced the value of friction coefficient from 0.5-0.7 to 0.006-0.15. Sanjari et al. [12] used FE to calculate the stress field in the radial forging process of the 6082 alloy at different operating conditions and compare with the experimental results obtained by the micro hardness test. In addition, the effects of various process parameters such as friction, die angle, axial feed, back push and front pull forces on the strain field were investigated. Findings have shown that the heterogeneity of deformation decreases with increase in die angle and decrease in back push and friction.

Although there have been many studies corresponding to forming or determining mechanical properties of aluminum alloys in the literature, no study has been conducted on the manufacturability of aluminum bushes with EN AW 6082. In addition to the effect of pretreatment conditions of EN AW 6082 on final product surface quality is unknown. In order to fill this gap in the literature, EN AW 6082 alloy is considered on the basis of pretreated conditions H13 (strain-hardened) and T4 (solution annealing and naturally aged). The effect of H13 and T4 on the final product surface quality was investigated by experimental and computer aided engineering studies.

II. MATERIALS AND EXPERIMENTAL PROCEDURE

2.1. Materials

In this study, Ø24 EN AW 6082 (AlSi1MgMn) alloy supplied by Drahtwerk ELISENTAL GmbH and chemical composition is given in Table 1. The alloy was produced in the form of wirerod by continuous casting and was prepared as pretreated H13 and T4.

Specimens were prepared by machining to be used in compression and extrusion tests.

Table 1. Chemical composition of the EN AW 6082 alloy used in the present study.

Si	Fe	Cu	Mn	Mg	Zn	Ti	Al
0.7-1.30	<0.50	<0.10	0.40-1.0	0.60-1.20	<0.20	<0.10	Balance

2.2. Experimental procedure

Compressive tests have been carried out to determine the flow curves of EN AW 6082 alloy at different temperatures and different strain rates. Cylindrical samples with a diameter of 8 mm and a length of 12 mm were prepared in accordance to ASTM E9-89 standard for compression tests and Zwick / Roell Z600 universal tester was used in the tests. Compression tests were carried out at nominal strain rates of 0.001, 0.1 s^{-1} and at temperatures of 20, 100 and 200 °C. The force-displacement curves were transformed into stress-strain curves firstly and then true stress-true plastic strain curves were drawn. Finally, the data is defined to Simufact. forming commercial FE software. The simulations of the compression tests were carried out at different temperatures and different strain rates to verify the models and compared with the experimental data. In addition to the strain rates used in the tests, the simulations were repeated at the average forging machine strain rate (approx. 50 s^{-1}). The simulation model of the compression test is shown in **Figure 1.**

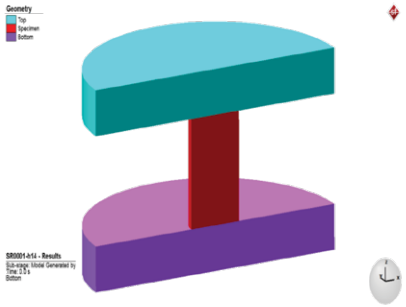

Figure 1. Compression simulation model.

Test and simulation studies were carried out to determine the behavior of EN AW 6082 alloy during extrusion. Samples with a diameter of 21.65 mm and a length of 40 mm were prepared for the extrusion tests and Zwick / Roell Z400 mechanical tester was used. In addition, the sticking phenomenon during the process was investigated. The technical drawing of the WC-Co die used in the extrusion tests is given in Figure 2. The extrusion ratio of in this die is 0.494 (49.4%) and hydraulic forging grease was used as lubricant.

Test and simulation studies were carried out to determine the behavior of EN AW 6082 alloy during extrusion. Samples with a diameter of 21.65 mm and a length of 40 mm were prepared for the extrusion tests and Zwick / Roell Z400 mechanical tester was used. In addition, the sticking phenomenon during the process was investigated. The technical drawing of the WC-Co die used in the extrusion tests is given in Figure 2. The extrusion ratio of in this die is 0.494 (49.4%) and hydraulic forging grease was used as lubricant.

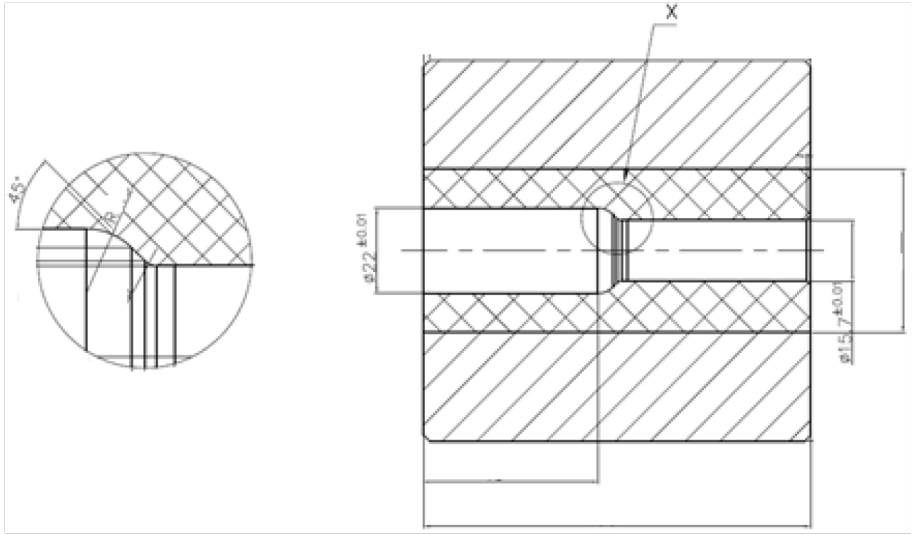

Fig. 2 Technical drawing of the extrusion die.

After identifying the flow stress curves and sticking behavior of the EN AW 6082 alloy with material conditions H13 and T4, cold forging station design was modeled in the Simufact.forming FE software and the prototype production was performed. In these experiments Hyodong HNP 627 cold forging machine with a capacity of 300 tons was used. In the study, Zeiss Stemi 508 stereo-zoom microscope was used for macroscopic examinations and surface roughness analyzes were performed on Ambios Technology XP-2 high-resolution surface profilometer.

III.RESULTS AND DISCUSSIONS

The engineering stress-strain curves of the EN AW 6082-H13 and EN AW 6082-T4 are given in Figures 3 (a) and 3 (b), respectively. It was found that EN AW 6082-H13 showed lower stress values and the yield stress of the H13 decreased with increasing temperatures. Although the stress values of EN AW 6082-T4 decrease due to increase in temperature, it is not as high as H13. In particular, no significant decrease in the yield stress of T4 was observed. In addition to these results, an increase in the stress values of H13 was observed with an increase of the quasi-static strain rate by about 100 times at room temperature. However, the increase in strain rates caused an adverse effect in T4 and decrease in stress value was occurred. The yield stress of H13 was found to be 140 MPa at room temperature, 130.6 MPa at 100 °C and about 107 MPa at 200 °C. The yield stress value of T4 was determined to be 130 MPa.

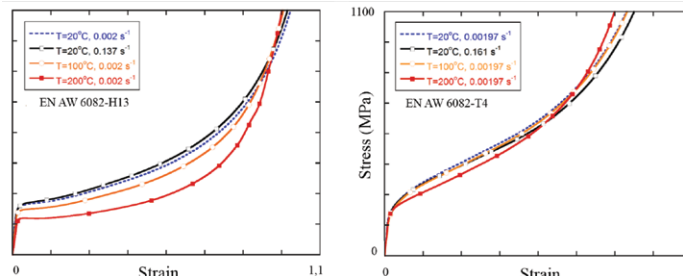

Fig. 3 Stress-strain curves of EN AW 6082 alloy; (a) H13, (b) T4.

The comparison of the experimental results with the simulations of EN AW 6082-H13 and EN AW 6082-T4 at different strain rates at room temperature is given in Figure 4. Simulations and experiment results are in quite good agreement. It has been found that the temperature in the sample rises to 150 °C at high strain rate (50 s-1). This temperature increase in the sample caused a decrease in the force values for EN AW 6082-H13 due to increase in temperature is more dominant than the increase in strain rate. However, there is no significant change in force values for T4 despite the increase in temperature and strain rate.

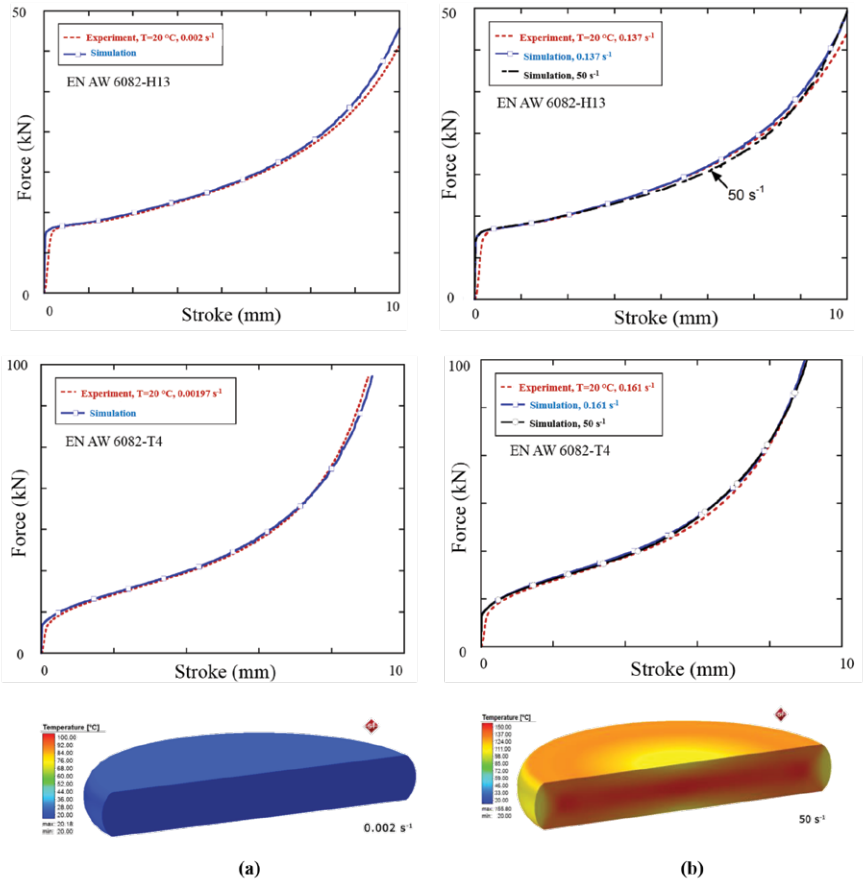

Fig. 4 Simulation results and temperatures in the samples for EN AW 6082-H13 and T4; (T=20 °C)

(a) $\dot{\varepsilon}$ =0.002 s^{-1} **(b)** $\dot{\varepsilon}$ =0.137 s^{-1} - 50 s^{-1}.

Figure 5 shows the surface condition on the samples after extrusion. Defects in the form of ripples were identified on the extrusion surfaces for pretreated H13 and T4. After the tests it was seen that the material chips were accumulated in the shoulder region of the extrusion die. Therefore, surface defects are estimated to be due to sticking phenomenon. On specimens of H13, surface defects begin at the shoulder region and condense at the shaft, however the defects is found to be distributed over the entire surface and more intense on T4 specimens. These findings are consistent with effective plastic strain values.

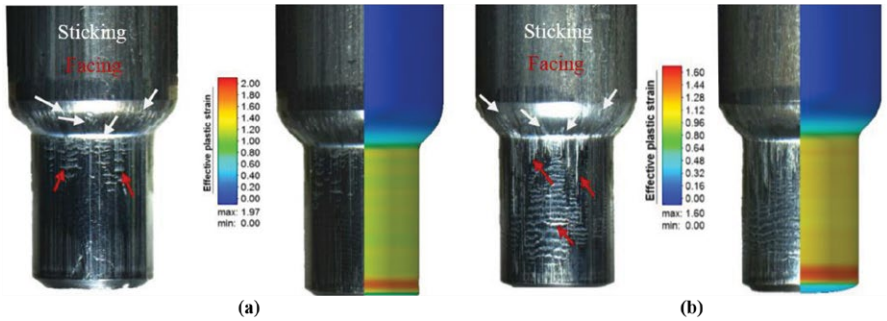

Fig. 5 Material surface condition after extrusion and effective plastic strain distributions; (a) EN AW 6082-H13 (b) EN AW 6082-T4

At the last stage of the work, aluminum bushes production trials were carried out. Figure 6 shows the cold forging station design and station samples. Bushes are manufactured by deforming the workpiece in consecutive forging stations. Therefore, each station has a different design and a different forming steps take place. The aluminum bushes were successfully manufactured with the EN AW 6082 alloy with both H13 and T4 conditions without experiencing any forming failure or fracture.

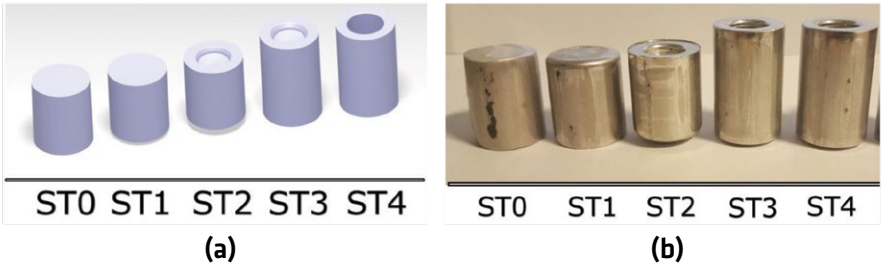

Fig. 6 Aluminum bushes (a) station design (b) station samples.

The prototypes were examined macroscopically and surface condition of the EN AW 6082-H13 and EN AW 6082-T4 were compared. According to Figure 7, it is observed that the final product surface qualities are different from each other and it was found that the amount of facing on the surface of bushes produced with EN AW 6082-T4 alloy is higher than EN AW 6082-H13.

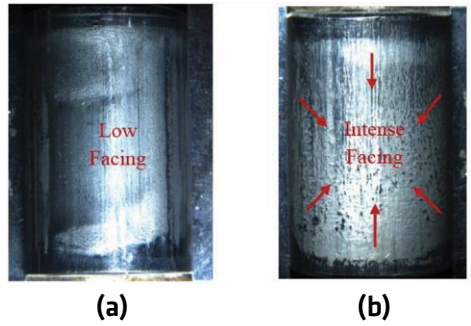

Fig. 7 Macroscopic examination of bushes produced with EN AW 6082 (a) H13 (b) T4.

In addition, the roughness parameters are comparatively measured so that the surface qualities of the aluminum bushes produced with EN AW 6082-H13 and EN AW 6082-T4 can be analytically evaluated. The values are given in Table 2 and the corresponding curves are given in Figure 8. When comparing the surface roughness parameters for H13 and T4, values are compatible with extrusion test results and macroscopic examinations. The Ra value for T4 is about 3-4 times greater than H13 and was measured as 3.81 µm.

Table 2. Surface roughness parameters of bushes produced with EN AW 6082-H13 and T4.

Pretreated Conditions	Surface Rougness Parameters (µm)			
	R_a	R_q	R_t	R_z
H13	0.99	1.26	8.99	6.80
T4	3.81	4.73	31.59	21.46

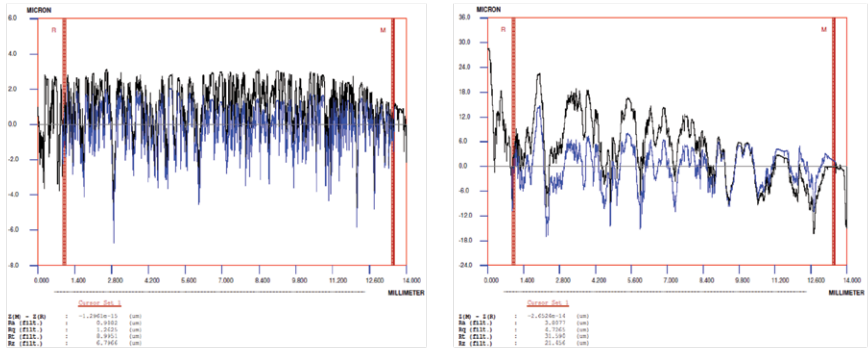

Fig. 8 Surface roughness curves of bushes produced with EN AW 6082 (a) H13 (b) T4.

CONCLUSIONS

In this study, the manufacturability of Ø23x36 aluminum bushes with pretreated EN AW 6082 (H13 and T4) was investigated. Flow stress curves were determined by compressive tests. Also, material flow and sticking behavior were determined by extrusion tests and roughness parameters were obtained with high resolution surface profilometer. The obtained results were compared with the FE analysis and confirmed.

According to results:

- EN AW 6082-H13 has a higher sensitivity to temperature than T4. Compression test results at different temperatures showed that, the yield stress of H13 was found to change between 140 MPa and 107 MPa. No significant change was observed in T4.
- Stress value of H13 increased with increasing strain rate. However, a decrease in T4 was observed.
- Compression simulations were carried out at the strain rates observed in cold forging machines (50 s-1) and the temperature in the sample reached 150 °C. It was determined that the softening observed due to the temperature increase was more dominant than strain hardening due to the high strain rate for H13 and the decrease in the force values was found. However, no significant change was observed for T4.
- The surface defects is found to be distributed over the entire surface and more intense on T4 specimens after extrusion tests.
- Ø23x36 aluminum bushes was produced successfully in production trials with both H13 and T4.
- It was calculated that Ra parameter of the cold forged H13 and T4 bushes as 0.99 µm and 3.81 µm, respectively.

ACKNOWLEDGMENTS

The authors thanks to employees of NORM CIVATA Co. and NORM SOMUN Co.

REFERENCES

[1]Jensrud O, Pedersen K. Cold forging of high strength aluminum alloys and the development of new thermomechanical processing, J Mater Process Technol 1998; 80–81:156–60.

[2]Birol Y, Ilgaz O, Akdi S, Unuvar E. Comparison of cast and extruded stock for the forging of AA6082 alloy suspension parts, Adv. Mater. Res. 2014; 939: 299–304.

[3]Oh SI, Wu WT, Tang JP. Simulations of cold forging processes by the deform system, Journal of Materials Processing Technology 1992; 35: 357-370

[4]European Union. Regulation (EC) No 443/2009 of the European Parliament and of the Council setting emission performance standards for new passenger cars as part of the Community's integrated approach to reduce CO2 emissions from light-duty vehicles, 2009.

[5]Kleiner M, Geiger M, Klaus A. Manufacturing of Lightweight Components by Metal Forming, CIRP Annals - Manufacturing Technology 2003; vol. 52, pp. 521-542.

[6]Tekkaya AE, Khalifa NB, Grzancic G, Hölker R. Forming of lightweight metal components: Need for new technologies, Procedia Engineering 2014; 81: 28 – 37.

[7]Davies G. Materials for automotive bodies. 2nd ed., 2012.

[8]Jeswiet J, Geiger M, Engel U, Kleiner M, Schikorra M, Duflou J. Metal forming progress since 2000, CIRP J Manuf Sci Technol 2000; 1: 2–17.

[9]Davis JR. Aluminum and Aluminum Alloys. ASM Specialty Handbook, ASM International, Materials Park, OH, 1996.

[10]Kuhlman GW. Forging of Aluminum Alloys, vol.14, ASM Handbook, 9th ed., ASM Int.1988, pp. 244–254.

[11]Bouquerel J, Diawara B, Dubois A, Dubar M, Vogt JB, Najjar D. Investigations of the microstructural response to a cold forging process, Materials and Design 2015; 68: 245–258.

[12]Geoffroy N, Vittecoq E, Birr A, de Mestral F, Martin J-M. Fatigue behaviour of an arc welded Al–Si–Mg alloy. Scr Mater 2007; 57: 349–52.

[13]Tveiten B, Fjeldstad A, Harkegard G, Myhr O, Bjorneklett B. Fatigue life enhancement of aluminium joints through mechanical and thermal prestressing, Int J Fatigue 2006; 28: 1667–76.

[14]Ishikawa T, Ishiguro T, Yukawa N, Goto T. Control of thermal contraction of aluminum alloy for precision cold forging, CIRP Annals - Manufacturing Technology 2014; 63: 289–292.

[15]Anjabin N, Taheri AK. The effect of aging treatment on mechanical properties of AA 6082 alloy: modeling and experiment, Iranian Journal of Materials Science & Engineering, 2010, Vol. 7, N.2.

[16]Wang P, Jiang H, Zhang R, Huang S. Study of Hot Deformation Behavior of 6082 Aluminum Alloy, Materials Science Forum 2016; 877: 340-346.

[17]Bay N, Eriksen M, Tan X, Wibom O. A friction model for cold forging of aluminum, steel and stainless steel provided with conversion coating and solid film lubricant, CIRP Annals - Manufacturing Technology 2011; 60: 303–306.

[18]Dubar L, Pruncu CI, Dubois A, Dubar M. Effects of contact pressure, plastic strain and sliding velocity on sticking in cold forging of aluminium billet, Procedia Engineering 2014; 81: 1842 – 1847.

[19]Sanjari M, Saidi P, Taheri AK, Zadeh MH. Determination of strain field and heterogeneity in radial forging of tube using finite element method and microhardness test, Materials and Design 2012; 38: 147–153.

PREVENTING HEAD CRACKS ON BOLTS: A NUMERICAL APPROACH

Tayfur YAVUZBARUT
Ph.D. Cenk KILIÇASLAN

Fastener Poland

PREVENTING HEAD CRACKS ON BOLTS: A NUMERICAL APPROACH

Tayfur Yavuzbarut
Ph.D. Cenk Kılıçaslan

Norm Civata San. ve Tic. A.Ş., Turkey (Norm Fasteners)

ABSTRACT

Cold forging, one of the oldest methods of production, is a metal forming process that is often preferred in today's industry. In cold forging process, workpiece is formed by being exposed to press forces between two dies or tools. Moreover, high surface quality can be obtained and precise tolerances can be achieved in cold forging.

The power of simulation applications has risen in the industry in the last decade due to their high predictive ability in all applied disciplines, especially in metal forming operations. The most important factor for improving product quality and cutting down costs is to use simulation applications in cold forging. Furthermore, there is a huge usage area including the detection of a defective product, material flow, tool stresses and post-mechanical features of the final part. In this paper, a crack problem on a round head with 12-lobe socket bolt was investigated. The source of the problem was determined by running simulations and then the results were compared to experimental results. Numerical simulations were prepared in the simufact.forming finite element software. This study also shows how the simulation software can be used in cold forging operations effectively.

HEAD CRACKING

The cold forging operation includes severe plastic deformation which is applied by forging presses at high speeds. The workpiece is formed at room temperature, however, forged material may be over the critical line of its fracture strength during deformation.
The M8x22 round head bolts were forged from the annealed 23MnB4 steel on a forging press of the maximum capacity of 70 tonnes in Norm Fasteners Co. The forging sequence of the bolts consists of 3 stations performing reduction, pre-heading and upsetting operations as shown in fig. 1. The technical drawing of the moving part of the station 3 die system is shown
in fig. 2. The moving side includes a N10 punch, a round-headed die and a die holder.

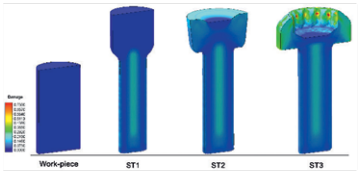

Fig 1. Forging sequence of the bolt

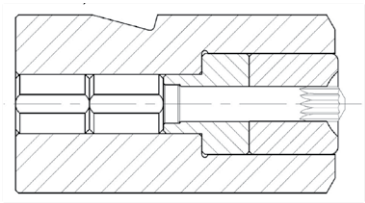

Fig 2. Technical drawing of the moving part

Cracks on head were seen at the 3th station as depicted in fig. 3. While this punch was forming the head, the material reached the fracture limit and macro-cracking occurred. In the beginning, the cracking mechanism was investigated by running a simulation at boundary conditions which are the same with as the real production conditions. It was seen that the crack formation on the head was also predicted in the numerical model as shown in fig. 4.

Fig 3. Cracks on the head

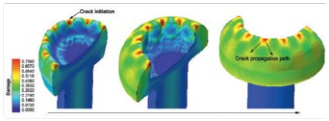

Fig 4. Cracks on the head in a simulation

According to these results, the cause of cracking is linked to the improper pre-heading form in the 2nd forging station. As shown in fig. 5, the diameter of the pre-heading form is slightly smaller than the diameter of the punch. The graph which shows the distribution of damage in the fracture area was shown in fig. 6. As it can be seen, both curves are over the damage limit of the steel.

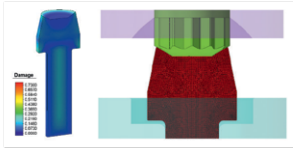

Fig 5. The 2nd forging station

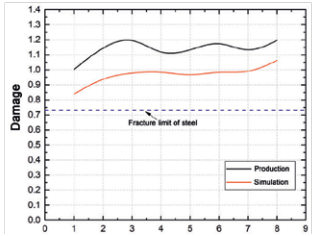

Fig 6. The damage – stroke graph

SOLUTION

At the beginning of the forging process, it has been determined by simulation software that the crack initiation was triggered from the corner of the socket. To eliminate a sharp corner evolution on the preform, the design of the 2nd station was completely altered as depicted in fig. 7. The simulation was run again with the revised dies for verification. Fig. 8 shows the distribution of the damage values on the head in the last situation. With the increase of the pre-head diameter, the amount of material contacting
the punch increases and the resulting stress spreads over a wider area. Thus, a sharp edge formation on the head was avoided and the damage values decreased accordingly as shown in fig. 9. The damage values were decreased around 0.5 ± 0.1% which is below
the fracture limit. According to these results, the die design of the bolt was revised and a production trial was conducted. As seen
in fig. 10, the crack evolution was completely eliminated.

fig 10.

CONCLUTION

In this paper, a crack problem on a round
head with 12-lobe socket bolt was investigated by using finite element sim ulations. The damage evolution on the head of the bolt was compared within different designs. For this purpose, the preform design of the bolt was revised. It was observed that the damage values
were reduced about 43% with the proper modifications of the pre-heading stage design. The production trial also proved the final design and the crack formation was completely avoided.

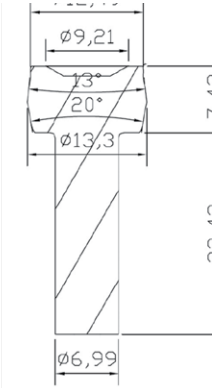

Fig 7. The revised 2nd station

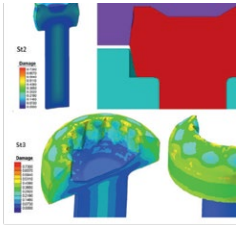

Fig 8. Simulation with the revised dies

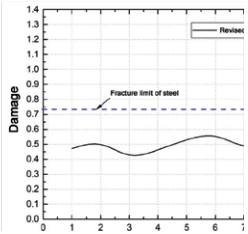

Table 9. The damage – stroke graph

PREDICTING MATERIAL FRACTURE IN COLD FORGING

Cenk KILIÇASLAN

The International Journal of
Forging Business & Technology (Forge Magazine)

Predicting Material Fracture in Cold Forging

Cenk Kılıçaslan

Norm Cıvata San. ve Tic. A.Ş., Turkey (Norm Fasteners)

ABSTRACT

Care should be taken in modeling the cold forging of fasteners through computer simulations. It has been shown that pre-forming operations have a significant effect on predicting cracking based on mathematical damage models. Pre-forming operations such as wire drawing and bar cropping should be included in the simulation model for highest accuracy and best predictive results.

Cold forging is a tough forming operation for mechanical component or fastener design that has limitations on the deformability of the workpiece material and tool life. In contrast to warm- and hot-forging processes, the deforming forces in cold forging are relatively high. Consequently, cold-forged material may have a tendency to crack due to the high deformation that exceeds the material's ductility limit. Because it is hard to detect failed cold-forged products during production, fastener manufacturers can suffer from high rates of wasted raw material and press energy. To eliminate this problem, the accuracy of predictive modeling on fracture evolution during forging is crucial in order to decrease manufacturing and engineering costs. The effects of pre-forging operations like wire drawing and bar cropping on computer simulations of fracture evolution are discussed in this article.

Fig. 1 Coils

PRE-FORGING OPERATIONS

Cold-forging materials (low- and medium-carbon steel alloys) were bought as coils from suppliers as shown in Figure 1. After the appropriate surface preparation (cleaning and phosphate coating), a wire-drawing operation was performed on each coil to eliminate any deviation from the desired circular cross-sectional shape. The diameter of the wire is reduced to 0.25-0.35 mm.
Figure 2 shows the inside of a forging press.

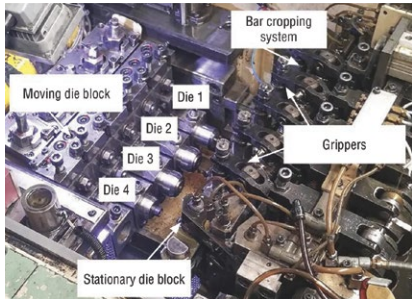

Fig. 2 Forging-press components

As depicted, basic press components are moving relative to the stationary die blocks, forging-die stations on these blocks, grippers and the bar- cropping mechanism. The wire coil is attached to the press and fed automatically through the bar-cropping system by the rolls. Wire is then cropped to the predetermined workpiece length and passed off to the first gripper. The grippers are mechanical components that transfer the workpiece and pre-forms between forging stations. During bar cropping, wire is constrained in a die while another die shears the material (Fig. 3). Here, shear and tensional stresses are dominant, and deformation is ductile. Engineers usually begin their forging simulations with the initial forging station. In most cases, this gives a sufficiently accurate prediction on material flow and forging forces. However, this modeling strategy may be deceptive for engineers who want to conduct failure analysis. An example of a fractured bolt that was taken from serial production is shown in Figure 4. As seen in the picture, cracking initiated from the corners of the 12-lobe punch and propagated through the head of the bolt. The crack's shape shows that this was caused by the forging operation. One can simply analyze this phenomenon using a finite-element simulation and predict the location of the crack's origin (Fig. 5). In some analyses the crack and its path may not be as obvious as that in Figure 5, however. In such a case, the simulation and fracture model may not predict the fracture evolution or exact fracture locus. At this point, the modeling of pre-forging operations plays a critical role on prediction accuracy. The engineer should go back to the first step of the forming operation and analyze it step by step.

MODELING PRE-FORGING OPERATIONS

Finite-element simulation software packages, such as the Lematrie, Cockroft-Latham, Oyane and Johnson-Cook damage models,
use different types of fracture and damage models. Most of the models use plastic effective strain for the damage calculation. At this point, calculation of exact values of generated plastic effective strain becomes important. When an engineer starts with the first forging step in a numerical model, he or she simply ignores the residual strain that comes from the wire-drawing operation. As shown in Figure 6, wire drawing generates moderate plastic strains on the surface of the workpiece material. Taking this into account, we see that the calculated damage value will be significantly affected by these surface strains, thus leading to better predictive capability. The next step that should be included in the simulation is bar cropping, which includes the drawn wire, the cropping die and the stationary die (Fig. 7). This analysis was carried out in Simufact forming finite-element software.

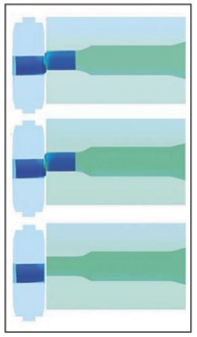

Fig. 3 Damage distribution of cold-forged bolt

Fig. 4 Fracture on cold-forged bolt

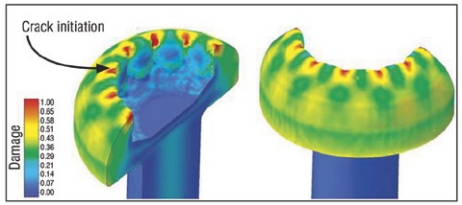

Fig. 5 Damage distribution of cold-forged bolt

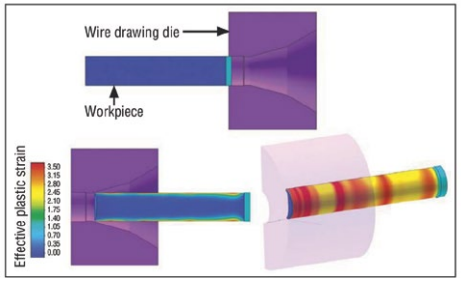

Fig. 6 Effective plastic-strain distribution on workpiece after the wire-drawing process

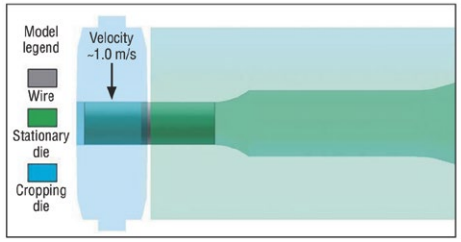

Fig. 7 Bar-cropping model

Damage distribution after the cropping operation is shown in Figure 8. There are two important findings from this model. The first is that on the cropped surface the maximum damage value is about 0.35 at the center of the workpiece and decreases to zero through the surface (Figs. 8 and 9). Similarly, the maximum effective plastic strain was generated on the center of the workpiece, and it is about 0.5. The second finding is that the geometrical deviation of the workpiece from a perfect cylindrical shape was determined as shown in Figure 9. This occurs due to ductile deformation during cropping. Including this geometrical deviation to the first forging station is also important to determine surface planarity of the bolt during forging. In most fracture cases in bolt cold forging, about 90% cracking is observed on the head of the bolt due to the forming of flanges or punch sockets. Here, crack evolution may be the result of a material defect or severe plastic deformation during forging. To investigate the damage on the head section of a pre-form bolt, an extrusion simulation was conducted using a workpiece taken from a bar-cropping model (along with the pre-forging model). The result of this simulation was then compared to the results of the extrusion model, in which the workpiece was simply drawn and taken to the model from CAD directly (without the pre- forging model). Figures 10 and 11 show the damage distribution on the extruded workpiece for simulations carried out with cropped and CAD workpieces. As shown in Figure 10, the average damage value on the head section is about 0.3, although the damage value of the same location without the pre-forging model is about zero (Fig. 11). The variations of damage value through the center to the surface on extruded parts are shown in Figure 12. Though the damage distribution tendency is similar for both models, the difference of generated damage on the head between these models is huge. This graph proves that an engineer who wants to conduct a failure analysis on a failed bolt and uses a simulation model without pre-forging models will underestimate the critical damage value on the fracture area and cannot gain reliable insight from simulation.

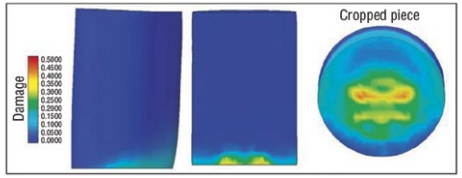

Fig. 8 Damage distribution on cropped workpiece

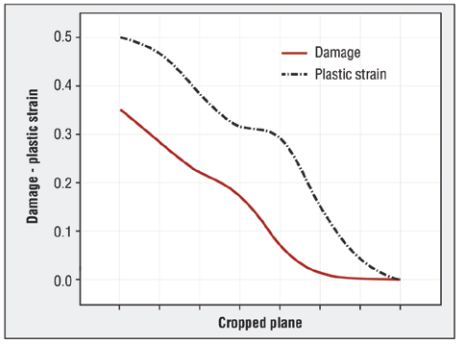

Fig. 9 Variation of damage and effective plastic strain on cropping zone

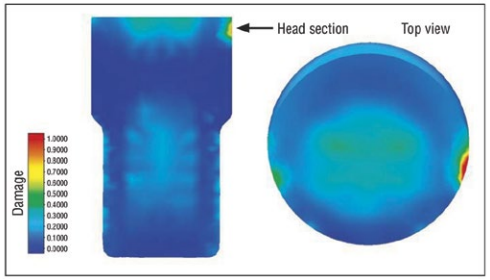

Fig. 10 Damage distribution on extruded part (with pre-forging model)

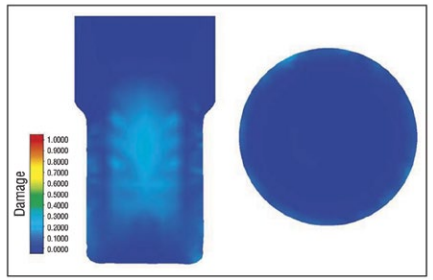

Fig. 11 Damage distribution on extruded part (without pre-forging model)

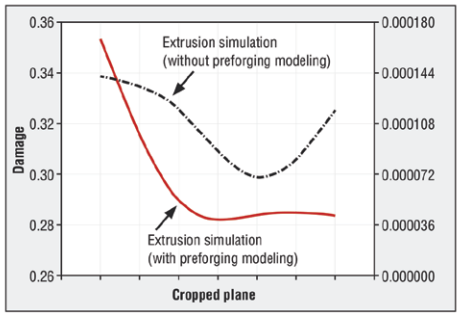

Fig. 12 Comparison of damage on simulations with and without pre-forging model

CONCLUSION

The accuracy of finite-element simulations depends on many variables, including material properties, geometrical accuracy of CAD models, finite-element type and distribution. Even if all parameters in a metal-forming simulation were defined to the software properly, however, the model may not give any reliable data. An engineer could come across this type of problem during the failure analysis of fractured products. This article shows that pre-forming operations have a significant effect on predicting cracking based on mathematical damage models. Metal-forming operations like wire drawing and bar cropping should be included in the forging simulation model for high accuracy even though this requires more computational time.

NORM
FASTENERS

www.normfasteners.com